

Influence of initial soil moisture in a Regional Climate Model study over West Africa. Part 1: Impact on the climate mean.

Brahima KONÉ¹, Arona DIEDHIOU^{1, 2}, Adama Diawara¹, Sandrine Anquetin², N'datchoh Evelyne Touré¹, Adama Bamba¹, and Arsene Toka Koba¹

¹LASMES, African Centre of Excellence on Climate Change, Biodiversity and Sustainable Agriculture / University Félix Houphouët Boigny, Abidjan, Côte d'Ivoire

²Univ. Grenoble Alpes, IRD, CNRS, Grenoble INP, IGE, F-38000 Grenoble, France

Correspondence to: Arona DIEDHIOU (arona.diedhiou@ird.fr)

Abstract.

The impact of initial soil moisture conditions on the mean climate over West Africa was examined using the latest version of the Regional Climate Model of the International Centre for Theoretical Physics (RegCM4) at a horizontal resolution of 25 km × 25 km. We performed these sensitivity studies on the initial conditions of soil moisture for June-July-August-September (JJAS) of two contrasted years 2003 (above normal precipitation year) and 2004 (below normal precipitation year). The soil moisture reanalysis of the European Centre Meteorological Weather Forecast's reanalysis of the 20th century (ERA20C) was used to initialize the control runs, whereas we initialized the soil moisture to the maximum and minimum value on our West African studied domain, corresponding to dry and wet initial soil moisture conditions respectively (hereafter dry and wet experiments). The impact of initial soil moisture condition on precipitation in West Africa is linear over the central and west Sahel where dry (wet) experiments lead to rainfall decrease (increase). The strongest precipitation increase is found over the West Sahel in wet experiments with a maximum change value of approximately +40%, while the strongest precipitation decrease is found in dry experiments over Central Sahel with a peak of change of approximately 4%. The sensitivity of anomalies in initial soil moisture condition can persist for three to four months (90-120 days) depending on the region. However, the influence on precipitation is no longer than one month (between 15 and 30 days). The strongest temperature decrease is located over the central and west Sahel with a maximum change of approximately -1.5 °C in wet experiments, while the strongest temperature increase is found over the Guinea coast and central Sahel in dry experiment with a maximum of change

33 around +0.6°C. A significant impact of initial soil moisture on the surface energy fluxes is
34 observed in the wet (dry) experiments with a cooling (warming) of the surface temperature, an
35 increase (decrease) sensible heat flux, a decrease (increase) of latent heat and an increase
36 (decrease) of the boundary layer depth over the study area, with different magnitudes varying
37 from one sub-region to another. Part II of this study investigates the influence of initial soil
38 moisture initial conditions on climate extremes.

39 **1 Introduction**

40 In the climate system, soil moisture is a crucial variable that influence water balance and surface
41 energy components through latent surface fluxes and evaporation. Therefore, soil moisture
42 impacts the development of weather patterns and precipitation production. The strength of soil
43 moisture impacts on land-atmosphere coupling varies according to location and season. Koster et
44 al. (2004) sustained that the atmospheric response simulation to the slow variation of the ocean
45 and land surface states, can improve seasonal simulations. The atmospheric response to ocean
46 temperature anomalies has been well documented (Kirtman et al. 1998; Rasmusson et al.1982).
47 Another potentially useful earth system component that varies slowly is soil moisture. Schär et
48 al. (1999) sustained that the role of soils may be comparable to that of the oceans. The solar
49 energy received by the oceans is stored in summer and used to heat the atmosphere in winter.
50 The precipitation received by the soils is stored in winter and contributed to moisten and cool the
51 atmosphere in summer. Through its impact on surface energy fluxes and evaporation, there are
52 many additional impacts on the climate process of soil moisture, such as boundary-layer stability
53 and air temperature (Hong and Pan, 2000; Kim and Hong 2006). Several studies have shown
54 that the anomalies of soil moisture may persist for several weeks or months, however, its impact
55 remains only for a shorter time in the atmosphere, not exceeding few days (Vinnikov and
56 Yeserkepova 1991; Liu et al., 2014). One important role of anomalies in soil moisture in the
57 coupling of land and atmosphere has been shown in several studies, using numerical climate
58 models (Jaeger et al., 2011; Zhang et al., 2011) and observation datasets (Zhang et al., 2008a;
59 Dirmeyer et al., 2006).

60 West Africa is known to exhibit strong coupling between soil moisture and precipitation (Koster
61 et al., 2004). Several previous studies have been conducted over West Africa on a global scale
62 using atmospheric general circulation model (AGCMs) to investigate the impact on the land-
63 atmosphere coupling of soil moisture anomalies (Koster et al., 2004; Douville and al, 2001;
64 Zhang et al., 2008b). However, at local and regional scales, the land-atmosphere coupling studies
65 with AGCM, present significant uncertainties (Xue et al. 2010). Recently, RCMs have been used

66 to simulate the impact on interannual climate variability of anomalies in soil moisture which has
67 received a lot of attention because of the increase in climate variability associated with extreme
68 weather events that can have greater societal and environmental impacts. In general, these
69 studies have been conducted in Asia, Europe and America (e.g. Seneviratne et al. 2006 for
70 Europe; Zhang et al. 2011 for Asia; Zhang et al. 2008b for America). Overall, the results of these
71 studies show that, during summer, the strong impact of the anomalies of soil moisture in land-
72 atmosphere occurred mainly over the transition zones with a climate between wet and dry
73 climate regimes. The relevance and extent of this potential feedback are still poorly understood
74 in West Africa. This study will focus on the influence of initial soil moisture conditions
75 anomalies on climate mean and it is based on performance assessment of the Regional Climate
76 model version 4 coupled to the version 4.5 of the Community Land Model (RegCM4-CLM4.5)
77 performed by Koné et al. (2018) where the ability of the model to reproduce the climate mean
78 has been validated. This study aims to estimate the limits of the impact of internal forcing of
79 initial soil moisture over West Africa region using a Regional Climate Model. Experiments
80 carried out are sensitivity studies that give idealized results of the effect of the initial soil
81 moisture. In this study (part I), the sensitivity of mean climate simulation to initial "wet" and
82 "dry" soil moisture conditions is investigated. In part II of the article, the influence of initial soil
83 moisture conditions on climate extremes will be explored. The descriptions of the model and
84 experimental setup used in this study are presented in Section. 2; in the Section 3, the influence
85 of the anomalies in soil moisture initial conditions on the subsequent climate mean is analyzed
86 and discussed; and in Section 4 the main conclusions are presented.

87 **2. Model and experimental design**

88 **2.1 Model description and observed datasets**

89 The fourth generation of the Regional Climate Model (RegCM4) of the International Centre for
90 Theoretical Physics (ICTP) was used in this study. Since its release, its physical
91 representations have been continuously developed and implemented. The version used in the
92 present study was RegCM4.7. The MM5 (Grell et al., 1994) non-hydrostatic dynamical core
93 has been ported to RegCM without removing the existing hydrostatic core. The model
94 dynamical core used in this study was non-hydrostatic. RegCM4 is a limited area model using
95 a sigma pressure vertical grid and the finite differencing algorithm of Arakawa B-grid (Giorgi
96 et al., 2012). The radiation scheme used in this version of RegCM4.7 is derived from the
97 National Center for Atmospheric Research (NCAR) Community Climate Model Version three
98 (CCM3) (Kiehl et al., 1996). Aerosols representation was taken from Zakey et al. (2006) and

99 Solmon et al. (2006). The large-scale precipitation scheme was taken from Pal et al. (2000)
100 and the moisture scheme is the SUBgrid EXplicit moisture scheme (SUBEX). The SUBEX
101 takes into account the sub-grid scale cloud variability, the accretion processes and evaporation
102 for stable precipitation following the work of Sundqvist et al. (1989). In the planetary
103 boundary layer (PBL), the sensible heat over ocean and land, water vapour and turbulent
104 transport of momentum are calculated according to the scheme of Holtslag et al. (1990). Heat
105 and moisture, the momentum fluxes of ocean surfaces in this study are computed as in Zeng et
106 al. (1998). In RegCM4.7, convective precipitation and land surface processes can be
107 described by several parameterizations. Based on Koné et al. (2018), we selected the
108 convective scheme reported by Emanuel (1991) and the interaction processes between soil,
109 vegetation and atmosphere are parameterized with CLM4.5. In each grid cell, CLM4.5 has 16
110 different Plant Functional Types (PFTs) and 10 soil layers (Lawrence et al., 2011; Wang et
111 al., 2016). RegCM4 was integrated over the domain of West Africa depicted in Fig. 1 with 25
112 km (182x114 grid points; from 20° W-20° E and 5° S-21° N) with horizontal resolution and
113 with 18 vertical levels and the initial and boundary conditions were taken from the European
114 Centre for Medium-Range Weather Forecasts reanalysis (EIN75; Uppala et al., 2008;
115 Simmons et al., 2007). The sea surface temperatures were obtained from the National Oceanic
116 and Atmosphere Administration (NOAA) optimal interpolation weekly (OI_WK) (Reynolds
117 et al., 1996). The topography data were taken from the States Geological Survey (USGS)
118 Global Multi-resolution Terrain Elevation Data (GMTED; Danielson et al., 2011) at 30 arc-
119 second spatial resolution, which is an update to the Global Land Cover Characterization
120 (GTOPO; Loveland et al., 2000) dataset.

121 Our analysis focused on precipitation and the 2 m air temperature over the West African domain
122 during the June-July-August-September (JJAS) summers in 2003 and 2004. Due to the coarse
123 resolution of the climate observing network over the region, we validated the simulated
124 precipitation based on two satellite derived products (Sylla et al., 2013a; Nikulin et al., 2012): the
125 TRMM datasets (Tropical Rainfall Measuring Mission 3B43V7) at the high-resolution 0.25°,
126 available from 1998 to 2013 (Huffman et al., 2007), and The Climate Hazards Group Infrared
127 Precipitation with Stations (CHIRPS) dataset developed at the University of California at Santa
128 Barbara at the 0.05° high-resolution available from 1981 to 2020. The validation of the simulated
129 2 m temperature relies on two observational datasets: the global daily temperature from the
130 Global Telecommunication System (GTS), gridded at 0.5° of horizontal resolution for 1979 to
131 2020 (Fan and van den Dool, 2008) and the CRU datasets (Climate Research Unit version 3.20)
132 from the University of East Anglia, gridded at a horizontal resolution of 0.5° for 1901 to 2011

133 (Harris et al., 2013). To facilitate comparison between RegCM4 simulations, all products were
134 re-gridded to $0.22^\circ \times 0.22^\circ$ using a bilinear interpolation method (Nikulin et al., 2012).

135 **2.2 Experiments setup and analysis methodology**

136 We designed an ensemble of three experiments, each with simulations starting from June 1st to
137 September 30th. The difference between these three experiments is the change in the initial soil
138 moisture condition during the first day of the simulation (June 1st). For each experiment, we
139 applied a (i) reference initial soil moisture condition, (ii) wet initial soil moisture condition, and
140 (iii) dry initial soil moisture condition.

141 We performed the simulations over 5 years (2001–2005) during the months of June to September
142 over the West African domain. We selected two extreme years (wettest and driest year) over the
143 study period to observe the estimates of the limits of the impact of internal soil moisture forcing
144 on the new dynamical core non-hydrostatic of RegCM4. In the same context, several previous
145 studies have selected two extreme years for their sensitivity study of initial soil moisture
146 conditions on the models. Hong and al. (2000) used only two years (three months per year) to
147 investigate the impact of initial soil moisture over North America (in the Great Plains) during
148 two summers spanning May-June-July (MJJ) in 1988 (corresponding to a drought) and 1993
149 (corresponding to a flooding event). Kim and Hong (2006) selected two contrasting years 1997
150 (below normal precipitation) and 1998 (above normal precipitation year) for their study over east
151 Asia. The first seven days (Kang et al., 2014) were excluded from the analysis as a spin-up
152 period.

153 With very little variation in soil moisture in one day, initial soil moisture conditions are given in
154 the first step of June 1 for JJAS 2003 and JJAS 2004. Except the geographical location, the
155 experimental setup is the same as that of Hong and Pan (2000). The geographical location of this
156 study is the same as in Koné et al. (2018), with four sub-regions (Fig. 1) exhibiting different
157 features of the annual precipitation cycle: Central Sahel (10° W - 10° E; 10° N - 16° N), west
158 Sahel (18° W - 10° W, 10° N - 16° N), and Guinea coast (15° W - 10° E; 3° N - 10° N). For each
159 year, three experiments were conducted. We used the soil moisture from the reanalysis of the
160 European Centre Meteorological Weather Forecast's reanalysis of the 20th century (ERA20C) to
161 initialize the control runs. We initialized the dry and wet soil moisture initial conditions (in
162 volumetric fraction $\text{m}^3.\text{m}^{-3}$) respectively at the minimum value ($=0.117*10^{-4}$) and the maximum
163 value ($=0.489$) derived from ERA20C dataset over the West African studied domain.

164 In several previous studies (Liu et al., 2014; Hong and Pan, 2000; Kim and Hong, 2006), the
165 mean biases (MB) averaged over their studied domains were used to quantify the impact of soil

166 moisture anomalies. In our study, we used the MB and probability density function (PDF; Gao et
167 al., 2016; Jaeger and Seneviratne, 2011) by fitting a normal distribution to better capture how
168 many grid points are impacted by initial soil moisture conditions. The pattern correlation
169 coefficient (PCC) was also used as a spatial correlation to reveal the degree of large-scale
170 similarity between model simulations and observations. We used two-tailed Student's t-
171 distribution to investigate the differences that were statistically significant at each grid cell
172 between the control and the sensitivity experiments (wet and dry). For the regional analysis such
173 as MB, PCC, and the PDF, both modeled and observed temperature and precipitation values
174 were calculated only over land grid points.

175

176 **3. Results and discussion**

177 **3.1. Influence of initial soil moisture conditions on precipitation.**

178 To identify the extreme years (driest and wettest) impacted by the dry and wet experiments
179 among the simulation period (2001–2005), we determined changes in daily soil moisture and
180 their climatological mean during JJAS over the West African domain from dry and wet
181 experiments with respect to their corresponding control experiment. These changes are presented
182 in Fig. 2, which shows that the weakest and strongest impacts of the dry experiments were
183 observed in 2003 and 2004, respectively. In a wet year, the impact of soil drying is quickly
184 erased. In a dry year, the impact of soil drying is accentuated. Thus, 2003 and 2004 are,
185 respectively, the wettest and driest years in the dry experiment. However, for the wet
186 experiments, the weakest impact was found for 2004, and the strongest impact was found for the
187 years 2001, 2002, and 2004. In a dry year, the impact of soil humidification is very quickly
188 mitigated, while in a wet year, the impact of soil humidification is accentuated. The wet
189 experiments confirmed the results obtained in dry experiments, demonstrating that 2003 and
190 2004 are the wettest and driest years, respectively. From this analysis, 2003 and 2004 were
191 selected to estimate the limits of the impact of internal soil moisture forcing on the new
192 dynamical core non-hydrostatic of RegCM4. Figure 3 displays the spatial distribution of the
193 observed mean rainfall (mm/day) from CHIRPS (Fig. 3a, d) and TRMM (Fig. 3b, e) for JJAS
194 2003 and JJAS 2004 and their corresponding simulated from control experiments (Fig. 3c, f)
195 initialized with reanalysis soil moisture ERA20C. Table 1 reports the MB and PCC for model
196 simulation and TRMM observation compared to CHIRPS, computed for the central Sahel,
197 Guinea coast, west Sahel, and the entire West African domain. The CHIRPS product displays a
198 zonal band of rainfall centered around 10° N, decreasing from north to south (Fig. 3a, d). The

199 maximum values are located over the mountain regions of Cameroun and Guinea. The TRMM
200 observations (Fig. 3b, e) are closer to CHIRPS and are quite similar to the North–South gradient
201 of precipitation with PCC up to 0.97 over the entire West African domain for both JJAS 2003
202 and JJAS 2004 (Table 1). However, although the observation datasets have similar large-scale
203 patterns, they exhibit differences at the local scale. CHIRPS shows a much larger extent of these
204 maxima than TRMM, especially over the Guinea highland and Cameroon mountains, while
205 TRMM shows a large band of precipitation that extends too far into the Sahel region. The
206 strongest MB between the two products are dry at approximately -15.45% and -16.96% ,
207 respectively, for JJAS 2003 and JJAS 2004 and are located over the Guinea coast sub-region
208 (Table 1). The control experiments (Fig. 3 c and f) initialized with the reanalyzed ERA20C soil
209 moisture effectively reproduced the large-scale pattern of observed rainfall with PCC 0.72 and
210 0.77 (Table 1), respectively, for JJAS 2003 and JJAS 2004 over the West Africa domain, despite
211 some biases at the local scale. The spatial extent of rainfall maxima and the North–South
212 gradient were well captured by control experiments; however, their magnitudes were
213 underestimated. In general, dry MB of app -49.31% and -50.56% were obtained for JJAS 2003
214 and JJAS 2004 over the whole West African domain (Table 1). Fig. 4 displays the change in
215 mean precipitation (in %) in JJAS 2003 and JJAS 2004 for dry and wet experiments with respect
216 to their corresponding control experiments. The dotted area shows changes with a statistical
217 significance of 0.05.

218 Dry and wet sensitivity experiments showed that precipitation was significantly affected by soil
219 moisture anomalies at varying degrees according to the sub-regions (Fig. 4). For the dry
220 experiments (Fig.4a, c), we found a dominant decrease in rainfall over the central Sahel
221 especially in JJAS 2003 and JJAS 2004 (Fig.4a and c). On the other hand, we found a dominant
222 increase in rainfall over the Guinea coast for both JJAS 2003 and JJAS 2004, and over the west
223 Sahel particularly in JJAS 2003. For the wet experiments (Fig.4b, d), there is a dominant
224 increase of rainfall over most of studied domains studied for both JJAS 2003 and JJAS 2004
225 (rep. Fig.4a and c). Overall, the impact of initial soil moisture conditions on the precipitation is
226 linear only over the central Sahel for both JJAS 2003 and 2004 and somewhat over the west
227 Sahel especially in JJAS 2004; that is, the dry (wet) experiments exhibits significant decrease
228 (increase) in precipitations with respect to the control experiments (Fig.4a, b).

229 For a better quantitative evaluation, the PDF distributions of precipitation changes in JJAS 2003
230 and JJAS 2004, over (a) central Sahel, (b) west Sahel, (c) Guinea coast and (d) West Africa
231 derived from dry and wet experiments compared to the corresponding control experiments are
232 shown in Fig. 5. Table 3 summarizes the maximum values of changes obtained on the PDF's of

233 this study. The impact of initial soil moisture on precipitation was not linear over most of the
234 studied domains (Fig.5 b-d) with the exception of central Sahel where the dry (wet) experiments
235 display significant decrease (increase) in precipitation with respect to the control experiments
236 (Fig.5a.). The strongest precipitation increase is found over west Sahel in wet experience in
237 JJAS 2004, and the maximum change is about 40%. However, the strongest precipitation
238 decrease is found over central Sahel in dry experiments in JJAS 2003 with a maximum change
239 value reaching -4% (Table 3). The impacts on precipitation from wet experiments were greater
240 than those from dry experiments (Table 3).

241 It is worth to note that, over the Guinea coast and the whole West African domain, for both dry
242 and wet experiments cause an increase of precipitation (Fig. 5c and d). The dry year had a
243 greater impact than the wet year in most of studied domains (Table 3). These results are
244 consistent with previous studies that supported a strong relationship between precipitation and
245 soil moisture in particular over the transition zones with a climate between wet and dry climate
246 regimes (Koster et al., 2004; Liu et al., 2014; Douville et al., 2001).

247 To better study the influence of soil moisture anomalies on precipitation for both dry and wet
248 years over the West African domain and its sub-regions, we analyzed changes in the daily
249 domain-average of soil moisture and precipitation (Fig. 6 and Fig. 7, respectively) for JJAS 2003
250 and JJAS 2004, from dry and wet experiments with respect to their corresponding control
251 experiments. The second soil layer in CLM4.5 (0 to 2.80 cm) corresponding to the top layer soil
252 moisture was used in this study. In general, soil moisture anomalies persist for three or four
253 months over the studied domains (Fig.6). Soil moisture anomalies disappeared for dry and wet
254 experiments with varying durations, between three to four months from one region to another
255 over the studied domain. The strongest duration and amplitude were found over the west Sahel
256 sub-region, for both wet and dry experiments, it lasted for four months in JJAS 2003 and JJAS
257 2004, although the signal was rather weak in the wet experiments compared with the dry ones
258 (Fig. 6b). A weaker change in soil moisture anomalies was found over the Guinea coast for wet
259 experiments and lasted three months (Fig. 6c). In dry experiments, a weaker change in soil
260 moisture anomalies was observed over central Sahel and lasted three months (Fig. 6a).

261 Figure 7 shows response of the daily precipitation to the initial soil moisture conditions over the
262 different studied domain. In general, the impact of the wet soil moisture anomalies on daily
263 precipitation is larger in magnitude than that of dry anomalies over most studied domains (Fig.
264 7). The strongest daily precipitation response in dry experiment ($-4\text{mm}\cdot\text{day}^{-1}$) is found over the
265 Guinea coast in the wet year JJAS 2003 (Fig. 7c), while for the wet experiments (more than
266 $8\text{mm}\cdot\text{day}^{-1}$, especially in JJAS 2003), it was found over the west Sahel and the Guinea coast

267 (Fig. 7b and c, respectively). However, the impact of initial soil moisture conditions on daily
268 precipitation is much shorter-lived than soil moisture change. A significant impact on daily
269 precipitation, greater than $1\text{mm}\cdot\text{day}^{-1}$ is only shown in wet experiments, and did not last more
270 than 15 days for most studied domains, except for the Guinea coast where it lasted
271 approximately one month. It is worth to note the peaks in precipitation over west Sahel and
272 Guinea coast (Fig. 7b and c, respectively) during August and September that coincide with
273 fluctuation in the anomalies of soil moisture (Fig.6b and c). This indicates that soil moisture and
274 precipitation feedback is strong during this period over the Guinea coast and west Sahel regions.
275 The response of the daily precipitation to initial soil moisture conditions anomalies is also
276 sensitive to wet and dry years. This is indicated by the lag between dry and wet experiments for
277 JJAS 2003 and JJAS 2004 years (Fig. 7). The magnitude of impacts due to contrasting years is
278 location dependent. For example, over Guinea coast, in the dry experiments, the wet year
279 presents a greater impact compared to the dry year (Fig.7 c). A reversed trend was observed for
280 central Sahel (Fig. 7a). These results are in line with previous works which argued that the soil
281 moisture-atmosphere feedback strength and the land memory are place dependent (Vinnikov et
282 al. 1996; Vinnikov and Yeserkepova 1991).

283 Fig. 8 and 9 show the vertical profile change in humidity and temperature for JJAS 2003 and
284 JJAS 2004, respectively, from dry and wet experiments over the entire West Africa domain and
285 its sub-region with respect to control experiments, as indicated in Fig. 1.

286 For the dry and wet experiments, the impact on humidity and temperature (Fig.8 and Fig.9) are
287 significant in the lower troposphere. The dry (wet) soil moisture experiments in the lower and
288 middle troposphere show drying (moistening) for humidity and warming (cooling) for
289 temperature. This indicates that for dry (wet) experiments a weak (strong) dry convection over
290 most of the studied domains (Fig.8 and Fig.9). The strongest impact on humidity and
291 temperature in the lower and middle troposphere is found over central Sahel (Fig.8a and Fig. 9a).
292 These results in the lower troposphere are consistent with the precipitation sensitivity, especially
293 over the central Sahel in JJAS 2003 (Fig. 4a, b). However, over west Sahel and the Guinea coast
294 this impact is somewhat low compared to that of central Sahel. In the dry experiments over the
295 Guinea coast (Fig.8c), these trends are reversed above 500 hPa for humidity, indicating wet
296 convection in this sub-region. These results in the lower atmosphere are consistent with the
297 precipitation sensitivity over the Guinea coast (Fig.4a, c).

298 On the over hand, in the upper troposphere, the significant impact on humidity and temperature
299 is found only for wet experiments, and exhibited a drying and warming respectively for humidity
300 and temperature over most of studied domains (Fig.8 and Fig.9). In the wet experiments, the

301 impact on upper tropospheric variability of initial soil moisture conditions anomalies which was
302 also reported by Hong and Pal (2000). The effect of soil moisture anomalies is mostly confined
303 to the near-surface and somewhat in the upper troposphere. Furthermore, in the upper
304 troposphere, relative humidity responses to initial soil moisture conditions anomalies are more
305 sensitive at atmospheric temperature to the contrast of the year, especially, in wet experiments
306 (Fig. 8 and Fig. 9).

307 To understand the causes of the precipitation changes illustrated in Fig. 4, we analyzed the lower
308 tropospheric wind (850hpa) and moisture changes for JJAS 2003 and JJAS 2004 from the dry
309 and wet experiments with respect to their corresponding control experiments; our findings are
310 presented in Fig. 10. In the dry experiments, we observed a dominant decrease of moistening
311 over most of studied domain; however, the strong wind magnitude change over the Atlantic
312 Ocean increase moisture from the ocean to the Guinea coast and west Sahel. This can explain the
313 increase precipitation over these sub-regions in the dry experiments. Over central Sahel, a weak
314 change in wind magnitude was observed, leading to strong decrease in precipitation which is
315 particularly notable in JJAS 2003 (Fig.4a). Conversely, for the wet experiments, an increase in
316 moistening was observed over most of studied domain. The strong change in wind magnitude
317 shifts the moistening from the north to the south, leading to increased precipitation over most of
318 domain studied in wet experiments (Fig.4 b and d). These results are broadly consistent with the
319 dry and wet precipitation changes shown in Figure 4.

320 Summarizing these results, the impact of initial soil moisture conditions anomalies was linear
321 only over the central Sahel for both JJAS 2003 and 2004 and over the west Sahel, especially in
322 JJAS 2004. The strongest precipitation decreasing (increasing) was observed over west Sahel
323 (central Sahel) in dry (wet) experiment in JJAS 2003 (JJAS 2004) with maximum change
324 reaching -4% (40%). The anomalies in initial soil moisture condition persist for three or four
325 months, while the significant impact on precipitation, greater than $1\text{mm}\cdot\text{day}^{-1}$, of the anomalies
326 in soil moisture is much shorter, no longer than one month. The anomalies in soil moisture
327 initial conditions effect are mostly confined to the near-surface climate and somewhat in the
328 upper troposphere.

329 **3.2. Influence on temperature and other surface fluxes.**

330 The spatial distribution of average temperature ($^{\circ}\text{C}$) from CRU (Fig.11 a and d) and GTS (Fig.11
331 b and e) observations for JJAS 2003 and JJAS 2004 and their corresponding mean temperature
332 simulated from control experiments (Fig.11 c and f) initialized with reanalysis soil moisture
333 ERA20C are shown in Fig.10. Table 2 summarizes the PCC and MB between the simulation of

334 the temperatures and CRU observation, calculated for the west Sahel, central Sahel, Guinea coast
335 and the entire West African domain.

336 The CRU temperature displays a zonal distribution over the whole West Africa domain.
337 Maximum values of approximately 34 °C were observed over the Sahara, and the lowest
338 temperatures were found on the Guinea coast especially in orographic regions such as Guinean
339 highlands, Cameroon mountains and the Jos Plateau, where the temperature did not exceed 26°C.
340 The two observation datasets GTS and CRU are similar at large spatial scale with PCC reaching
341 0.99 over the entire West African domain for both JJAS 2003 and JJAS 2004 (Table 2).
342 However, the extension and the amplitude of these maxima and minima are quite different in the
343 two sets of gridded observations. While GTS (Fig.11b and e) observation displays large (small)
344 areas with maximum (minimum) values, CRU (Fig. 11a and d) presents small (large) area of
345 these maxima (minima) values. The strongest mean warm biases between the two observation
346 products, reaching 0.54°C and 0.67°C respectively for JJAS 2003 and JJAS 2004, are located
347 over the west Sahel sub-region compared to the others sub-regions (Table 2). The control
348 experiments (Fig.11 c and f) show good agreement in the representation of the large-scale pattern
349 of the observed temperature (CRU) with PCC 0.99 for both JJAS 2003 and JJAS 2004 (Table 2),
350 including the zone of the meridional gradient of the surface temperature between Sahara Desert
351 and Guinea coast which is crucial for the African Easterly Jet evolution and formation
352 (Thorncroft and Blackburn 1999; Cook 1999). However, some biases were noted at the local
353 scale. The spatial extent of temperature maxima and minima are well reproduced by control
354 experiments, however their magnitudes were overestimated. The strongest warm MB of control
355 experiments with respect to CRU observation are approximately 2.68 °C and 2.14 °C
356 respectively for JJAS 2003 and JJAS 2004, are found over the West Sahel sub-region (Table 2).

357 Fig. 12 shows changes in mean temperature (°C) for JJAS 2003 and JJAS 2004, from dry and
358 wet experiments with respect to their corresponding control experiments. The dotted area shows
359 changes that are statistically significant at the 0.05 level. In the dry experiments, for both JJAS
360 2003 and JJAS 2004, the dominant warm changes are located over most of area under the
361 latitude 13° N, with maximum values located over the Guinea coast. On the other hand, for the
362 wet experiments, we found a dominant cool change over the west and central Sahel.

363 For a better quantitative evaluation, the PDF distributions of the changes in mean temperature in
364 JJAS 2003 and JJAS 2004, over (a) the central Sahel, (b) west Sahel, (c) Guinea and (d) West
365 Africa derived from dry and wet experiments with respect to their corresponding control
366 experiments are shown in Figure 13. The temperature impact is linear over the central Sahel,
367 Guinea coast and the whole West African domain (Fig.13a, c and d). The strongest mean

368 temperature decrease was observe over the central and west Sahel (JJAS 2004 and JJAS 2003,
369 respectively; Table3) in wet experiences with the maximum change approximately $-1.5\text{ }^{\circ}\text{C}$.
370 However, the strongest mean temperature increasing were found over the central Sahel (JJAS
371 2003) and the Guinea coast (JJAS 2004) in dry experiments reaching $0.56\text{ }^{\circ}\text{C}$ and 0.59°C
372 respectively(Table 3). Overall, the dry (wet) sensitivity experiments for 2m-temperature showed
373 a dominant increase (decrease) in warming (cooling) for both JJAS 2003 and JJAS 2004 over
374 most of the studied domains, except for the west Sahel, where both dry and wet experiments lead
375 to an increase of temperature (Fig.13, Table3).

376 We now analyze the influence of initial soil moisture conditions anomalies on land energy
377 balance, particularly on the surface fluxes sensible and latent heat. Figure 14 shows changes in
378 sensible heat fluxes (in W.m^{-2}) for JJAS 2003 and JJAS 2004, from dry and wet experiments
379 compared to their corresponding control experiments, and the dotted area shows changes that are
380 statistically significant at the 0.05 level. As shown in figure 14, initial soil moisture conditions
381 anomalies strongly affect the sensible fluxes. The impact on sensible heat of initial soil moisture
382 condition anomalies was linear over most of the studied domains, that is, the dry (wet)
383 experiments with respect to the control exhibits significant increase (decrease) of the sensible
384 heat (Fig.14).

385 The PDF distributions of change in sensible heat flux are displayed in Figure 15. The dry (wet)
386 experiments show an increase (decrease) of the sensible flux in both JJAS 2003 and JJAS 2004
387 over studied domains (Fig. 15). The impact in wet experiments was strong compared to the dry
388 experiments over central and west Sahel except over Guinea coast (Fig. 15, Table 3). The
389 strongest increasing (decreasing) in sensible heat flux was found over Guinea coast (central
390 Sahel) in dry (wet) experiments, with maximum change about 9.18 W.m^{-2} (-39.66 W.m^{-2}) in
391 JJAS 2004 (2003) (see Table 3).

392 Unlike the case of sensible heat flux, changes in latent heat show a linear opposite patterns, a
393 dominant decrease (increase) of latent heat flux is observed over most of studied domains in dry
394 (wet) experiment (Fig.16). The PDF distributions of latent heat flux change are shown in Figure
395 17. The results indicate that the impact on latent heat flux of soil moisture anomalies was linear,
396 that is, dry experiments result in a decrease in latent heat flux, while the wet experiments result
397 in an increase in the latent heat flux over most of studied domains. The strongest increase
398 (decrease) in latent heat flux was found in wet (dry) experiments over west Sahel (Guinea coast)
399 with maximum change reaching 36.49 W.m^{-2} (-14.64W.m^{-2}) in JJAS 2004(Table3). It is worth to
400 note that the impacts on latent and sensible heat flux in wet experiments are strong compared to
401 the dry experiments over most of studied domains, except over Guinea coast (Table 3).

402 To determine whether most changes in energy go to evaporating water or to heating the
403 environment, we analyzed the changes in Bowen ratio for JJAS 2003 and JJAS 2004, for dry and
404 wet experiments with respect to their corresponding control experiments, the results are provided
405 in Fig. 18. The dotted area displays statistically significant differences at the 0.05 level. The soil
406 moisture anomalies strongly affected the Bowen ratio. The dry (wet) experiments show a
407 dominant increase (decrease) of evaporation energy (Bowen ratio value in the range [0,1]) over
408 most studied domains, except over the west Sahel for both JJAS 2003 and JJAS 2004 (Fig.18).
409 As expected, the areas where most energy changes go to water evaporation are coincident with
410 areas of temperature changes. The decrease (increase) in the evaporation area coincides with the
411 decrease (increase) of temperature change.

412 For a quantitative evaluation, the PDF distribution of the Bowen ratio is shown in Figure 18. The
413 impact of initial soil moisture conditions on the Bowen ratio was linear over most studied
414 domain for both JJAS 2003 and JJAS 20004, except for west Sahel in JJAS 2003 (Fig. 18). The
415 dry (wet) experiments show an increase (decrease) of water evaporation energy. The strongest
416 increase (decrease) of energy going in evaporation is found over the central and west Sahel (over
417 the central Sahel and Guinea coast) in JJAS 2004, in the dry (wet) experiments with maximum
418 change reaching 0.39 and 0.41 (-0.64) respectively (Table 3). However, the strongest impact on
419 energy going to heat the environment is found over the west Sahel reaching -3.01 and -2.41 in dry
420 and wet experiments respectively.

421 We then examine the impact on the stability of the PBL of the anomalies in initial soil moisture
422 conditions. Soil moisture can influence rainfall by limiting evapotranspiration, which affects the
423 development of the daytime PBL and thereby the initiation and intensity of convective
424 precipitation (Eltahir, 1998). Fig. 20 shows changes in PBL (in m) for JJAS 2003 and JJAS
425 2004, from dry and wet experiments with respect to their corresponding control experiments
426 with dotted areas that are statistically significant at the 0.05 level. The anomalies in initial soil
427 moisture conditions impact significantly the PBL. The dry experiments demonstrated an
428 dominant increase in PBL under the latitude 15° N for both JJAS 2003 and JJAS 2004 (Fig.20 a
429 and c, respectively). For the wet experiments, a decrease in PBL is located over most of the
430 studied domains. The PDF distribution of PBL changes, computed over the area indicated in
431 Figure1 is shown in Fig. 21. The impact on PBL is linear over most of studied domains (Fig.21).
432 The dry (wet) experiments lead to an increase (decrease) of PBL for both JJAS 2003 and JJAS
433 2004 over most of studied domains. The strongest increase (decrease) in PBL was found over
434 Guinea coast (west Sahel) in dry (wet) experiments in JJAS 2004 (JJAS 2003) reaching 146.80m
435 (293.23m). There is dry (wet) air above the area where there is increase (decrease) in PBL,

436 which results in warm (cool) and dry (moist) over most studied domains (see Fig. 8 and Fig. 9).
437 These results are consistent with the work of Han and Pan 2003.

438 Summarizing the results of this section, in the wet experiments, the cooling of mean surface
439 temperature is associated with a decrease of latent heat flux, an increase in sensible heat flux and
440 the PBL depth over most of the studied domain. Conversely, in the dry experiments, the
441 warming of surface temperature is associated with an increase of the latent heat flux, a decrease
442 of the sensible heat flux and PBL height. These results are consistent with those of Eltahir et al.
443 (1998). Furthermore, sensible and latent heat fluxes, Bowen ratio and PBL responses to initial
444 soil moisture conditions the anomalies are somewhat sensitive to the contrast of year and
445 experiments (wet and dry).

446

447 **4. Conclusion**

448 The impact of initial soil moisture conditions anomalies on the subsequent summer mean climate
449 over West Africa was explored using the RegCM4-CLM45. In particular, the aim of this study
450 was to investigate how soil moisture initialization at the beginning of the rainy season may affect
451 the intraseasonal variability of temperature and precipitation mean within the subsequent season
452 (June to September). For this purpose, three experiments each with simulations beginning from
453 June 1st to September 30th were set up and runs were performed in JJAS 2003 and in JJAS 2004.
454 The difference between these 3 experiments is the change in initial soil moisture condition at the
455 beginning of the simulation: For each experiment, we applied a (i) control soil moisture initial
456 condition, (ii) wet soil moisture initial condition, and (iii) dry soil moisture initial condition.

457 The impact of initial soil moisture condition on precipitation depends on the location, magnitude
458 and persistence of initial soil moisture condition anomalies throughout the season. The impact of
459 initial soil moisture conditions anomalies was linear only over the central Sahel for both JJAS
460 2003 and 2004 over the west Sahel especially in JJAS 2004. The strongest precipitation decrease
461 (increase) is found over the central Sahel (over central Sahel) in dry (wet) experiment in JJAS
462 2003 (JJAS 2004) with maximum change reaching -4% (40%). Anomalies of initial soil
463 moisture condition can persist for three to four months (90-120 days) depending on the region of
464 West Africa but the impact on precipitation is no longer than 30 days (15 days over the Sahel
465 and 30 days over the Guinea Sahel).

466 Our results indicate that a wet soil moisture initial condition lead in the low levels of the
467 atmosphere to an increase of relative humidity associated with a cooling of temperature and in
468 the upper levels, to a decrease of relative humidity and a warming, while the dry experiment

469 mainly impact the lower levels with a decrease of the relative humidity associated with a
470 warming. However, over the West Sahel and Guinea coast, the increase of precipitation shown in
471 the dry experiments may result from the transport of moisture from the Atlantic Ocean by
472 westerlies. The temperature is more sensitive to the anomalies of initial soil moisture condition
473 than precipitation. The strongest impacts are located over the central Sahel with a maximum
474 change of approximately $-1.5\text{ }^{\circ}\text{C}$ and $0.6\text{ }^{\circ}\text{C}$ respectively in wet and dry experiments. Our study
475 showed significant impact of initial soil moisture conditions anomalies on the surface energy
476 fluxes. We observed in wet (dry) experiments that the cooling (warming) of surface temperature
477 was associated with an increase (decrease) of sensible heat flux, a decrease (increase) of latent
478 heat and an increase (decrease) of the depth of the boundary layer over the region, with different
479 magnitudes varying from one sub-region to another.

480 This study shows that soil moisture as a boundary condition plays a major role in controlling
481 summer climate variability not only over the transition zone of climate but also, over humid
482 zones such as Guinea coast. This study demonstrates that a good prescription of the initial
483 condition of soil moisture can improve the simulation of precipitation and air temperature, which
484 would help to reduce biases in climate model simulations. Overall, land surface initialization can
485 contribute to improving sub-seasonal to seasonal forecast skill, but this requires further
486 investigation. We recognize that sensitivity experiments such as "wet" and "dry" ones conducted
487 in this study were not intended to simulate real climate since such extremes are very rare. These
488 experiments, however, can facilitate estimation of the limits of internal forcing impact of soil
489 moisture on the new non-hydrostatic dynamical core of RegCM4. Finally, in the context of
490 climate change, considering the projected increase of high-impact weather events in the region,
491 there is a need to explore the sensitivity of initial soil moisture conditions to climate extremes.

492

493 **Authors contributions**

494 The authors declare to have no conflict of interest with this work. B. Koné and A. Diedhiou fixed
495 the analysis framework. B. Koné carried out all the simulations and figures production
496 according to the outline proposed by A. Diedhiou. Then B. Koné and A. Diedhiou, S. Anquetin
497 and A. Diawara worked on the analyses. All authors contributed to the drafting of this
498 manuscript.

499 **Acknowledgements**

500 The research leading to this publication is co-funded by the NERC/DFID "Future Climate for
501 Africa" programme under the AMMA-2050 project, grant number NE/M019969/1 and by IRD

502 (Institut de Recherche pour le Développement; France) grant number UMR IGE Imputation
503 252RA5.

504

505 **References:**

506

507 Beljaars A. C. M., Viterbo P. , Miller M. J., and Betts A. K.: The anomalous rainfall over the
508 United States during July 1993: Sensitivity to land surface parameterization and soil moisture
509 anomalies, *Mon. Weather Rev.*, 124(3), 362–382, doi:10.1175/1520-0493(1996)124<0362:
510 TAROTU>2.0.CO;2, 1996.

511

512 Bosilovich, M. G., and Sun W. Y.: Numerical simulations of the 1993 Midwestern flood: Land–
513 atmosphere interactions. *J. Climate*, 12, 1490–1505, 1999.

514

515 Cook K. H.: Generation of the African easterly jet and its role in determining West African
516 precipitation, *J. Climate*, 12, 1165–1184, [https://doi.org/10.1175/1520-0442](https://doi.org/10.1175/1520-0442(1999)012) (1999)012
517 <1165:GOTAEJ> 2.0.CO;2, 1999.

518

519 Danielson J.J., and Gesch D.B.: Global multi-resolution terrain elevation data 2010
520 (GMTED2010): U.S. Geological Survey Open-File Report 2011–1073, 26 p, 2011.

521

522 Dirmeyer P. A., Koster R. D., and Guo Z.: Do global models properly represent the feedback
523 between land and atmosphere?, *J. Hydrometeorol.*, 7(6), 1177–1198, doi:10.1175/JHM532.1,
524 2006.

525

526 Douville, F. Chauvin, and H. Broqua.: Influence of soil moisture on the Asian and African
527 monsoons. Part I: Mean monsoon and daily precipitation. *J. Climate*, 14, 2381–2403, 2001.

528

529 Eltahir E. A. B.: A soil moisture-rainfall feedback mechanism 1. Theory and observations, *Water*
530 *Resour. Res.*, 34, 765–776, doi:10.1029/97WR03499, 1998.

531

532 Emanuel K. A.: A scheme for representing cumulus convection in large-scale models. *Journal of*
533 *the Atmospheric Science* 48: 2313–2335, 1991.

534

535 Fan Y., and van den Dool H.: A global monthly land surface air temperature analysis for 1948 -
536 present, *J. Geophys. Res.* 113, D01103, doi: 10.1029/2007JD008470, 2008.

537

538 Gao, X.-J., Shi, Y., and Giorgi, F.: Comparison of convective parameterizations in RegCM4
539 experiments over China with CLM as the land surface model, *Atmos. Ocean. Sci. Lett.*, 9, 246–
540 254, <https://doi.org/10.1080/16742834.2016.1172938>, 2016.

541

542 Giorgi F., Coppola E., Solmon F., Mariotti L., Sylla M. B., Bi X., Elguindi N., Diro G. T., Nair
543 V., Giuliani G., Cozzini S., Guettler I., O'Brien T., Tawfik A., Shalaby A., Zakey A. S., Steiner
544 A., Stordal F., Sloan L., and Brankovic C.: RegCM4: model description and preliminary tests
545 over multiple CORDEX domains, *Clim. Res.*, 52, 7–29, <https://doi.org/10.3354/cr01018>, 2012.

546

547 Grell G., Dudhia J. and Stauffer D. R.: A description of the fifth generation Penn State/NCAR
548 Mesoscale Model (MM5), National Center for Atmospheric Research Tech Note NCAR/TN-
549 398+STR, NCAR, Boulder, CO, 1994.

550

551 Harris I., Jones P. D., Osborn T. J. and Lister D. H.: Updated high-resolution grids of monthly
552 climatic observations, *Int. J. Climatol.*, 34, 623–642, <https://doi.org/10.1002/joc.3711>, 2013.

553

554 Holtslag A., De Bruijn E., and Pan H. L.: A high resolution air mass transformation model for
555 short-range weather forecasting, *Mon. Weather Rev.*, 118, 1561–1575, 1990.

556

557 Hong S-Y. and Pan H-L.: Impact of soil moisture anomalies on seasonal, summertime
558 circulation over North America in a regional climate model. *J. Geophys. Res.*, 105 (D24), 29
559 625–29 634, 2000.

560

561 Huffman G. J., Adler R. F., Bolvin D. T., Gu G., Nelkin E. J., Bowman K. P., Hong Y, Stocker
562 E. F., and Wolff D. B.: The TRMM multisatellite precipitation analysis: quasi-global, multi-year,
563 combined-sensor precipitation estimates at fine scale, *J. Hydrometeorol.*, 8, 38-55, 2007.

564

565 Jaeger E. B., and Seneviratne S.I.: Impact of soil moisture-atmosphere coupling on European
566 climate extremes and trends in a regional climate model, *Clim. Dyn.*, 36(9-10), 1919-1939,
567 doi:10.1007/s00382-010-0780-8, 2011.

568
569 Kang S, Im E.-S. and Ahn J.-B.: The impact of two land-surface schemes on the characteristics
570 of summer precipitation over East Asia from the RegCM4 simulations *Int. J. Climatol.* 34: 3986-
571 3997, 2014.

572
573 Kiehl J., Hack J., Bonan G., Boville B., Breigleb B., Williamson D., Rasch P. ; Description of
574 the NCAR Community Climate Model (CCM3). National Center for Atmospheric Research
575 Tech Note NCAR/TN-420+STR, NCAR, Boulder, CO, 1996.

576
577 Kim J-E., and Hong S-Y.: Impact of Soil Moisture Anomalies on Summer Rainfall over East
578 Asia: A Regional Climate Model Study, *Journal of Climate.* Vol. 20, 5732–5743, DOI:
579 10.1175/2006JCLI1358.1, 2006.

580
581 Kirtman B.P., Schopf P. S.: Decadal Variability in ENSO Predictability and Prediction. *Journal*
582 *of Clim.* 11, 2804, 1998.

583
584 Koné B., Diedhiou A., N’datchoh E. T., Sylla M. B., Giorgi F., Anquetin S., Bamba A., Diawara
585 A., and Koba A. T.: Sensitivity study of the regional climate model RegCM4 to different
586 convective schemes over West Africa. *Earth Syst. Dynam.*, 9, 1261–1278.
587 <https://doi.org/10.5194/esd-9-1261-2018>, 2018.

588
589 Koster R. D., Dirmeyer P. A., Zhichang G., Bonan G., Chan E., Cox P., Gordon C. T., Kanae
590 S., Kowalczyk E., Lawrence D., Liu P., Lu C. H, Malyshev S., McAvaney B., Mitchell K,
591 Mocko D., Oki T., Oleson K., Pitman A., Sud Y. C. , Taylor C. M., Verseghy D., Vasic R., Xue
592 Y., Yamada T.: Regions of strong coupling between soil moisture and precipitation, *Science*,
593 305, 1138–1140, doi:10.1126/science.1100217, 2004.

594
595 Lawrence D.M., Oleson K.W., Flanner M.G., Thornton P.E., Swenson S.C., Lawrence P.J. ,
596 Zeng X., Yang Z.-L., Levis S., Sakaguchi K., Bonan G.B., and Slater A.G.:Parameterization
597 improvements and functional and structuraladvances in version 4 of the Community Land
598 Model. *J. Adv. Model. Earth Sys.* 3. DOI:10.1029/2011MS000045, 2011.

599

600 Liu D., Wang G. L., Mei R., Yu Z. B. and Gu H. H.: Diagnosing the strength of land-atmosphere
601 coupling at sub-seasonal to seasonal time scales in Asia, *J. Hydrometeorol.*, doi:10.1175/JHM-D-
602 13-0104.1, 2013.

603

604 Liu D., Wang R. Mei Z. Yu, and Yu M.: Impact of soil moisture initial conditions anomalies
605 on climate mean and extremes over Asia, *J. Geophys. Res. Atmos.*, 119, 529–545,
606 doi:10.1002/2013JD020890, 2014.

607

608 Loveland, T. R., Reed, B. C., Brown, J. F., Ohlen, D. O., Zhu, J., Yang, L., and Merchant, J. W.:
609 Development of a global land cover characteristics database and IGBP DISCover from 1-km
610 AVHRR Data, *Int. J. Remote. Sens.*, 21, 1303–1330, 2000.

611

612 Oglesby R. J., and Erickson III D. J.: Soil moisture and the persistence of North American
613 drought. *J. Climate*, 2, 1362–1380, 1989.

614

615 Oglesby R. J., Marshall S., Erickson III D. J., Roads J. O. and Robertson F. R.: Thresholds in
616 atmosphere-soil moisture interactions: Results from climate model studies. *J. Geophys. Res.*, 107,
617 4244, doi:10.1029/2001JD001045, 2002.

618

619 Oleson K., Lawrence D. M., Bonan G. B., Drewniak B., Huang M., Koven C. D., Yang Z. -L.:
620 Technical description of version 4.5 of the Community Land Model (CLM) (No. NCAR/TN-
621 503+STR). doi:10.5065/D6RR1W7M, 2013.

622

623 Paeth H., Girmes R., Menz G. and Hense A.: Improving seasonal forecasting in the low latitudes,
624 *Mon. Weather Rev.*, 134, 1859-1879, 2006.

625

626 Pal J. S., Small E. E. and Elthair E. A.: Simulation of regional scale water and energy budgets:
627 representation of subgrid cloud and precipitation processes within RegCM, *J. Geophys. Res.*,
628 105, 29579–29594, 2000.

629

630 Pal J. S. and Elthair E. A. B.: Pathways relating soil moisture conditions to future summer
631 rainfall within a model of the land–atmosphere system. *J. Climate*, 14, 1227–1242, 2001.

632

633 Peterson T. C., Folland C., Gruza G., Hogg W. Mokssit A., Plummer N.: Report on the activities
634 of the working group on climate change detection and related rapporteurs 1998-2001. Geneva
635 (Switzerland): WMO Rep. WCDMP 47, WMO-TD 1071, 2001.
636

637 Nicholson S. E.: The West African Sahel: a review of recent studies on the rainfall regime and its
638 interannual variability, *Meteorology*, 453521, 32 p., <https://doi.org/10.1155/2013/453521>, 2013.

639 Nikulin G., Jones C., Samuelsson P., Giorgi F., Asrar G., Büchner M., Cerezo-Mota R.,
640 Christensen O. B., Déque M., Fernandez J., Hansler A., van Meijgaard E., Sylla M. B. and
641 Sushama L.: Precipitation climatology in an ensemble of CORDEX-Africa regional climate
642 simulations, *J. Climate*, 6057–6078, <https://doi.org/10.1175/JCLI-D-11-00375.1>, 2012.
643

644 Rasmusson E. M. and Carpenter T. H.: Variations in Tropical Sea Surface Temperature and
645 Surface Wind Fields Associated with the Southern Oscillation/El Niño. *Mon. Weather Rev.* 110,
646 354, 1982.
647

648 Reynolds, R. W. and Smith, T. M.: Improved global sea surface temperature analysis using
649 optimum interpolation, *J. Climate*, 7, 929–948, 1994.
650

651 Seager R., and Vecchi G. A.: Greenhouse warming and the 21st century hydroclimate of
652 southwestern North America. *Proc. Natl. Acad. Sci. USA*, 107, 21 277–21 282,
653 [doi:10.1073/pnas.0910856107](https://doi.org/10.1073/pnas.0910856107), 2010.
654

655 Simmons A. S., Uppala D. D. and Kobayashi S.: ERA-interim: new ECMWF reanalysis products
656 from 1989 onwards, *ECMWF Newsl.*, 110, 29–35, 2007.
657

658 Solmon F., Giorgi F., and Lioussse C.: Aerosol modeling for regional climate studies: application
659 to anthropogenic particles and evaluation over a European/African domain, *Tellus B*, 58, 51–72,
660 2006.
661

662 Sundqvist H. E., Berge E., and Kristjansson J. E.: The effects of domain choice on summer
663 precipitation simulation and sensitivity in a regional climate model, *J. Climate*, 11, 2698-2712,
664 1989.

665
666 Thorncroft, C. D. and Blackburn, M.: Maintenance of the African easterly jet, *Q. J. R. Meteorol*
667 *Soc.*, 125, 763–786, 1999.

668
669 Uppala S., Dee D., Kobayashi S., Berrisford P. and Simmons A.: Towards a climate data
670 assimilation system: status update of ERA-interim, *ECMWF Newsl.*, 15, 12–18, 2008.

671
672 Vinnikov K. Y. and Yeserkepova I. B.: Soil moisture: Empirical data and model results, *J. Clim.*,
673 4(1), 66–79, doi:10.1175/1520-0442(1991) 004<0066:SMEDAM>2.0.CO;2, 1991.

674
675 Vinnikov K. Y., Robock A., Speranskaya N. A. and Schlosser A.: Scales of temporal and spatial
676 variability of midlatitude soil moisture, *J. Geophys. Res.*, 101(D3), 7163–7174,
677 doi:10.1029/95JD02753, 1996.

678
679 Wang, G., Yu, M., Pal, J. S., Mei, R., Bonan, G. B., Levis, S., and Thornton, P. E.: On the
680 development of a coupled regional climate vegetation model RCM-CLM-CN-DV and its
681 validation its tropical Africa, *Clim. Dynam*, 46, 515–539, 2016.

682
683 Xue Y., De Sales F., Lau K. M. W., Bonne A., Feng J., Dirmeyer P., Guo Z., Kim K. M., Kitoh
684 A., Kumar V., Pocard-Leclercq I., Mahowald N., Moufouma-Okia W., Pegion P., Rowell D. P.,
685 Schemm J., Schulbert S., Sealy A., Thiaw W. M., Vintzileos A., Williams S. F. and Wu M. L.:
686 Intercomparison of West African Monsoon and its variability in the West African Monsoon
687 Modelling Evaluation Project (WAMME) first model Intercomparison experiment, *Clim.*
688 *Dynam.*, 35, 3–27, <https://doi.org/10.1007/s00382-010-0778-2>, 2010.

689
690 Zakey A. S., Solmon F., and Giorgi F.: Implementation and testing of a desert dust module in a
691 regional climate model, *Atmos. Chem. Phys.*, 6, 4687–4704, [https://doi.org/10.5194/acp-6-4687-](https://doi.org/10.5194/acp-6-4687-2006)
692 2006, 2006.

693
694 Zeng X., Zhao M. and Dickinson R. E.: Intercomparison of bulk aerodynamic algorithms for the
695 computation of sea surface fluxes using TOGA COARE and TAO DATA, *J. Climate*, 11, 2628-
696 2644, 1998.

697 Zhang, J., W.-C. Wang, and J. Wei, Assessing land-atmosphere coupling using soil moisture
698 from the Global Land Data Assimilation System and observational precipitation, *J. Geophys.*
699 *Res.*, 113, D17119, doi:10.1029/2008JD009807, 2008.

700 Zhang, J., W.-C. Wang, and L. R. Leung.: Contribution of land-atmosphere coupling to summer
701 climate variability over the contiguous United States, *J. Geophys. Res.*, 113, D22109,
702 doi:10.1029/2008JD010136, 2008.

703

704 Zhang, J. Y., L. Y. Wu, and W. Dong.: Land-atmosphere coupling and summer climate
705 variability over East Asia, *J. Geophys. Res.*, 116, D05117, doi 10.1029/2010JD014714, 2011.

706

707

708

709

710

711

712

713

714

715

716

717

718

719

720

721

722

723

724

725

726

727

728

729

730

731

732

733 **Tables and figures:**

734

	Central Sahel		West Sahel		Guinea		West Africa	
	PCC	MB (%)	PCC	MB (%)	PCC	MB (%)	PCC	MB (%)
TRMM 2003	0.98	7.60	0.96	-945	0.98	-15.45	0.97	-0.57
CTRL_2003	0.98	-47.97	0.87	-75.76	0.82	-47.12	0.73	-49.31
TMM 2004	0.98	-0.62	0.99	-7.03	0.98	-16.96	0.97	-1.56
CTRL_2004	0.98	-47.89	0.87	-68.35	0.85	-51.97	0.77	-50.56

735

736 **Table1:** The pattern correlation coefficient (PCC) and the mean bias (MB) for JJAS precipitation
737 for model simulation and observation TRMM with respect to CHIRPS, calculated for Guinea
738 coast, central Sahel, west Sahel and the entire West African domain during the period 2003 and
739 2004.

740

741

742

743

744

745

746

747

748

749
750
751
752

	Central Sahel		West Sahel		Guinea		West Africa	
	PCC	MB (°C)	PCC	MB (°C)	PCC	MB (°C)	PCC	MB (°C)
GTS 2003	0.99	0.31	0.99	0.54	0.99	0.28	0.99	0.39
CTRL_2003	0.99	1.52	0.99	2.68	0.99	-0.34	0.99	0.85
GTS 2004	0.99	0.32	0.99	0.67	0.99	0.28	0.99	0.40
CTRL_2004	0.99	1.50	0.99	2.14	0.99	-0.57	0.99	0.51

753

754 **Table2:** The pattern correlation coefficient (PCC) and the mean bias (MB) for JJAS 2m-
755 temperature for model simulation and observation (GTS) with respect to CRU, calculated for
756 Guinea coast, central Sahel, west Sahel and the entire West African domain during the period
757 2003 and 2004.

758

759

760

761

762

763

764

765

766

767

768

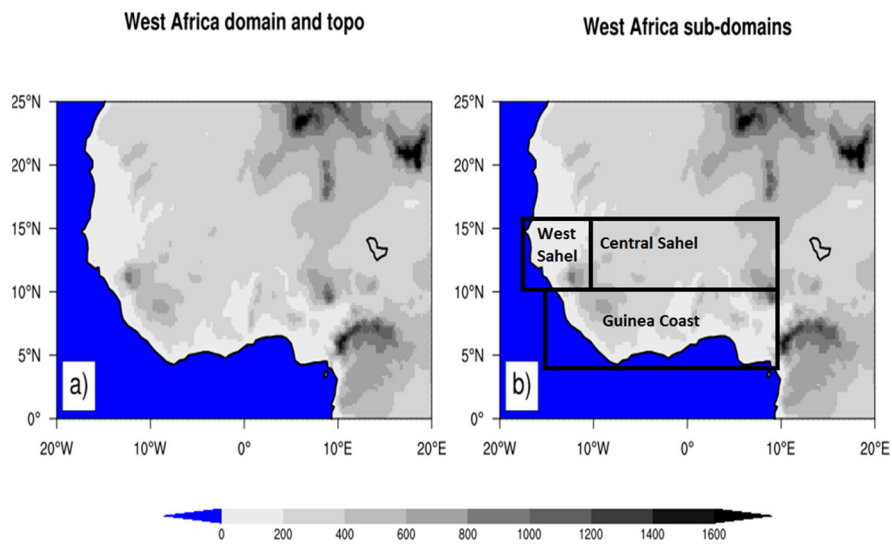
769

		Central Sahel		West Sahel		Guinea coast		West Africa	
		ΔWC	ΔDC	ΔWC	ΔDC	ΔWC	ΔDC	ΔWC	ΔDC
Precipitation (%)	2003	13.80	-4.09	29.95	6.58	19.40	9.20	8.88	4.68
	2004	15.86	-3.29	38.58	-1.25	26.6	12.68	10.72	7.64
Temperature mean (°C)	2003	-1.48	0.56	-1.55	-0.41	-0.15	0.54	-0.62	0.50
	2004	-1.51	0.47	-1.15	-0.24	-0.19	0.59	-0.41	0.59
Sensible heat (w.m ⁻²)	2003	-16.89	8.57	-39.66	5.31	-2.41	7.52	-14.32	8.06
	2004	-19.53	7.55	-31.97	7.23	-3.01	9.18	-14.46	6.81
Latent heat (w.m ⁻²)	2003	21.27	-6.67	34.21	-6.06	3.09	-13.38	15.86	-8.07
	2004	28.55	-4.81	36.49	-6.20	7.09	-14.64	19.68	-8.53
Bowen ratio	2003	-0.42	0.31	-3.01	-0.05	-0.03	0.12	-0.48	0.28
	2004	-0.64	0.39	-2.49	0.41	-0.64	0.15	-0.57	0.26
PBL	2003	-233.49	81.23	-293.23	-0.16	-94.42	132.74	-128.90	75.57
	2004	-223.06	49.48	-247.08	19.87	-119.38	146.80	-117.69	56.53

770

771 **Table3:** Table summarizing the maximum values of change obtained on the PDF distribution for
772 precipitation, temperature, sensible heat, latent heat, Bowen ratio and PBL, calculated for Guinea
773 coast, central Sahel, west Sahel and the entire West African domain during the period 2003 and
774 2004.

775



776

777

778 **Figure 1:** Topography of the West African domain. The analysis of the model result has an
779 emphasis on the whole West African domain and the three subregions Guinea coast, central
780 Sahel and west Sahel, which are marked with black boxes.

781

782

783

784

785

786

787

788

789

790

791

792

793

794

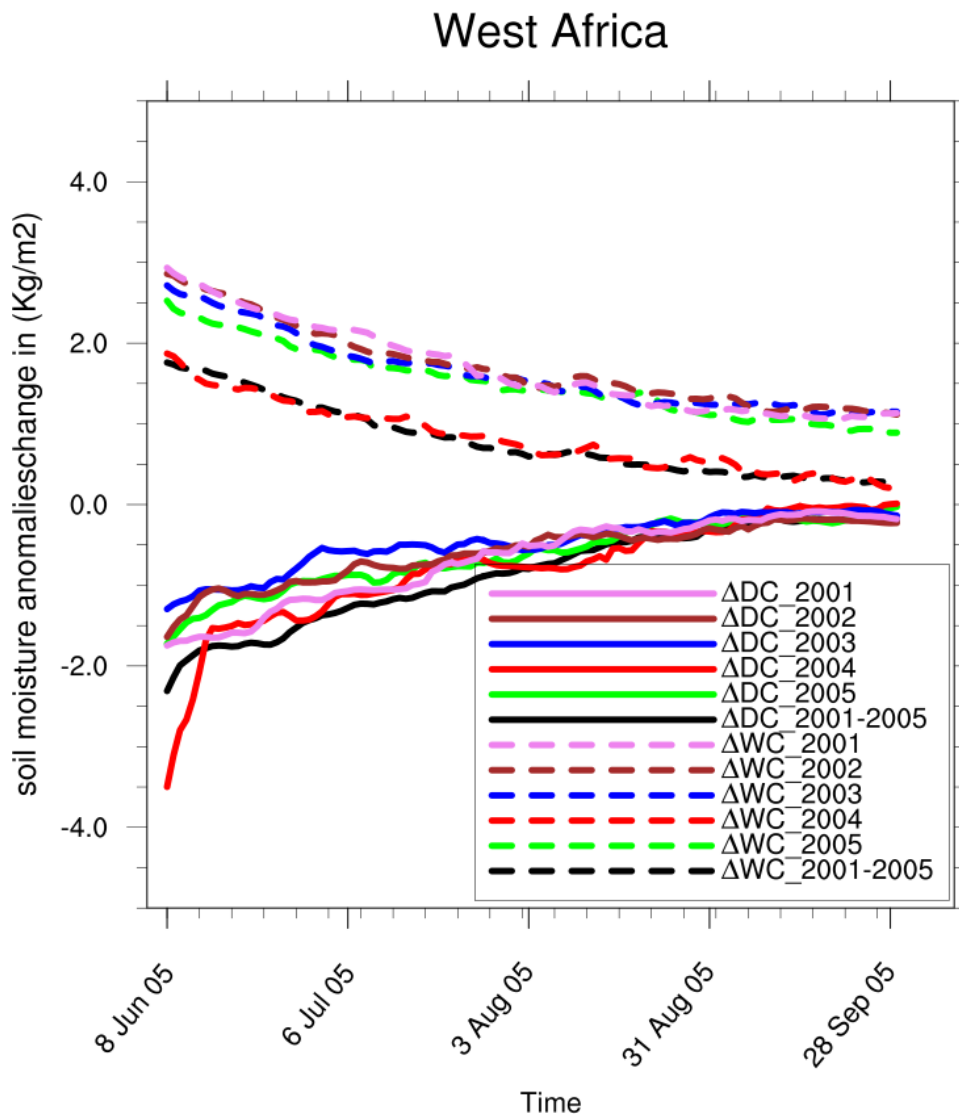
795

796

797

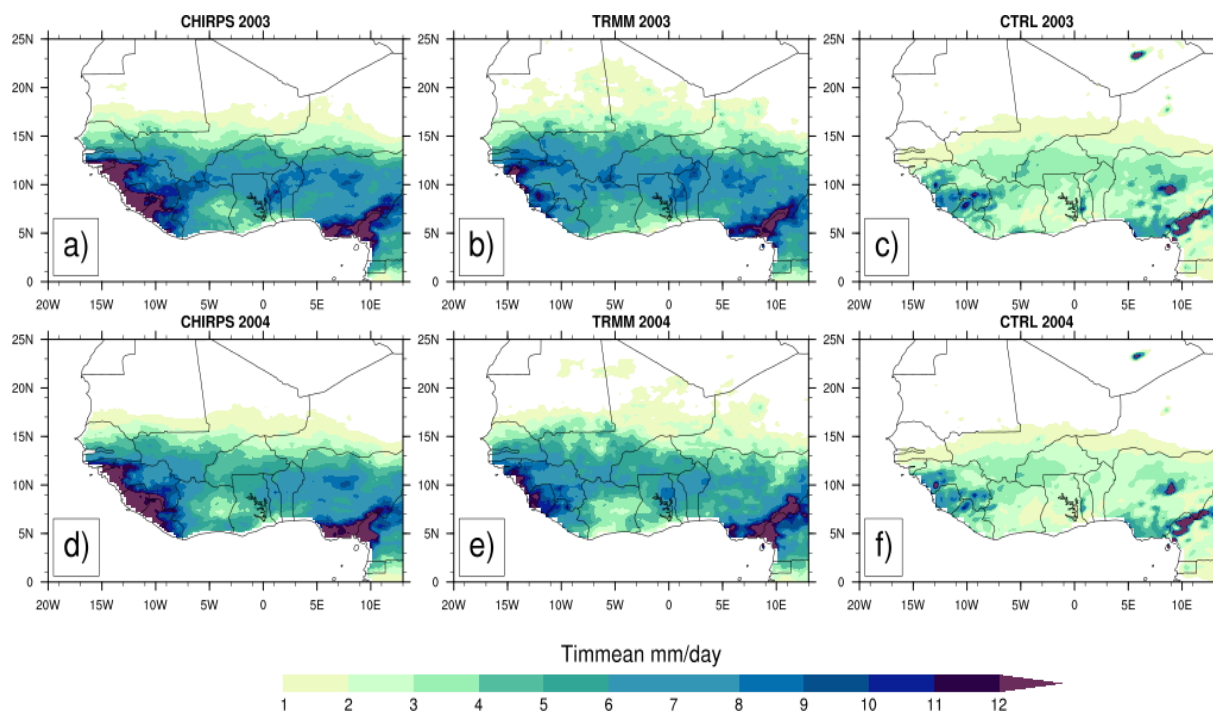
798

799
800
801



802
803 **Figure 2:** Changes in daily soil moisture for 5 years (2001 to 2005) and their climatological
804 mean during JJAS over West African domain, from dry (ΔDC) and wet (ΔWC) experiments with
805 respect to their corresponding control experiment.

806
807
808
809
810
811
812
813



814

815

816

Figure3: Observed 4-month averaged (JJAS) precipitation (mm/day) from CHIRPS (a and d) and TRMM (b and e) for 2003 and 2004 and their corresponding mean rainfall simulated control experiments (CTRL) (c and f) with the reanalysis initial soil moisture ERA20C.

819

820

821

822

823

824

825

826

827

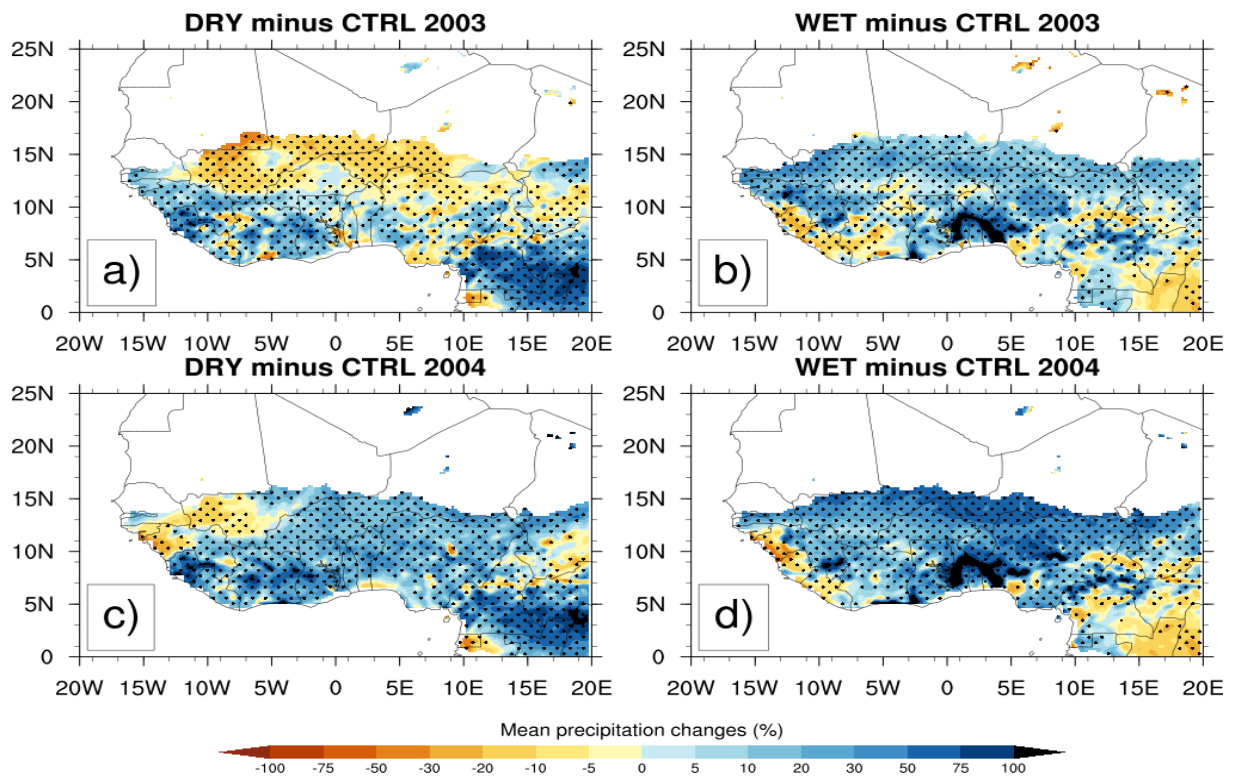
828

829

830

831

832



833

834

835 **Figure4:** Changes in mean precipitation (in %) for JJAS 2003 and JJAS 2004, from dry (resp. a
 836 and c) and wet (resp. b and d) experiments with respect to their corresponding control
 837 experiment, the dotted area shows differences that are statistically significant at 0.05 level.

838

839

840

841

842

843

844

845

846

847

848

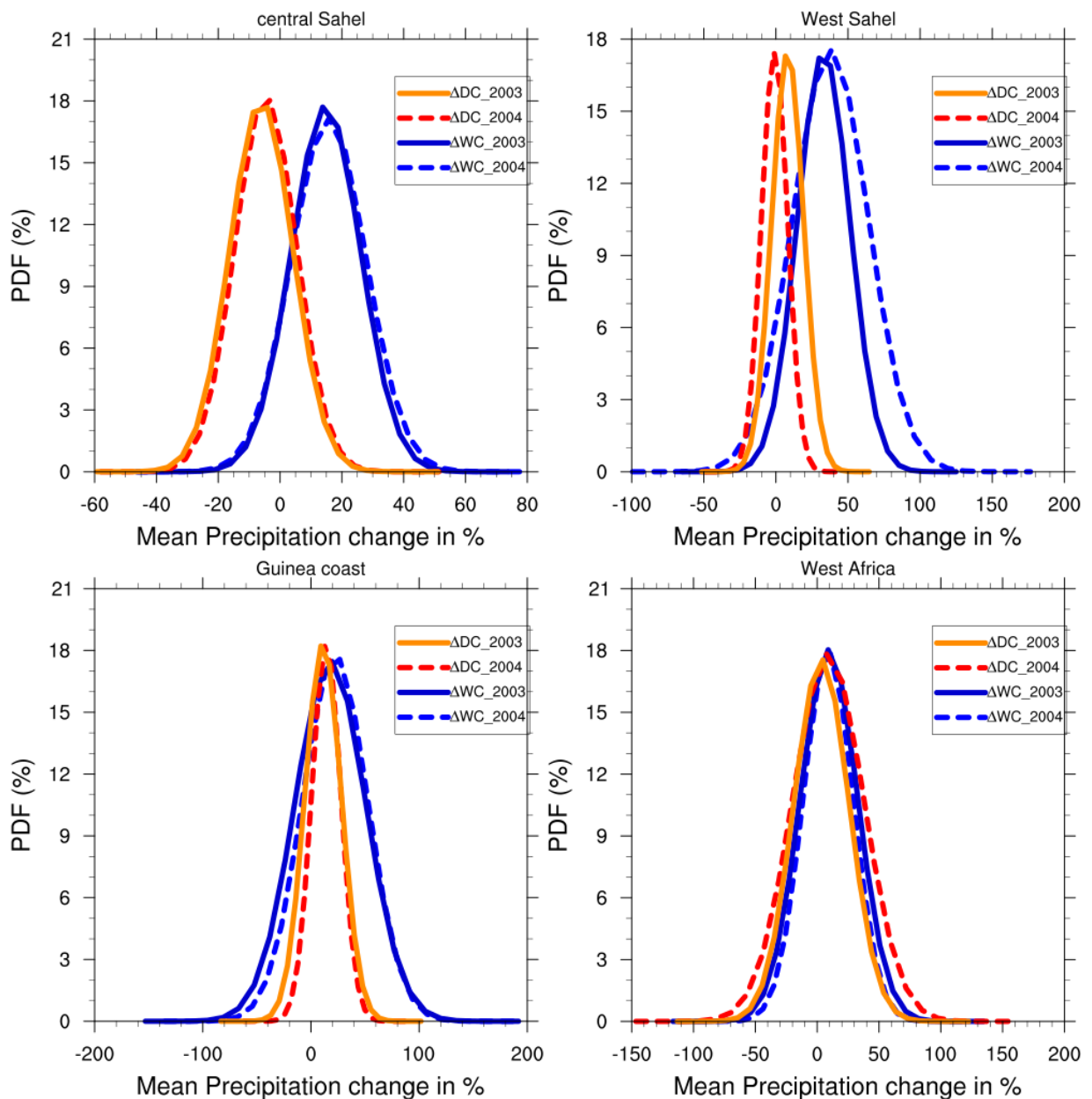
849

850

851

852

853



855
 856 **Figure 5:** PDF distributions (%) of mean precipitation changes in JJAS 2003 and JJAS 2004,
 857 over (a) central Sahel, (b) West Sahel, (c) Guinea and (d) West Africa derived from dry (ΔDC)
 858 and wet (ΔWC) experiments compared to their corresponding control experiment.

859

860

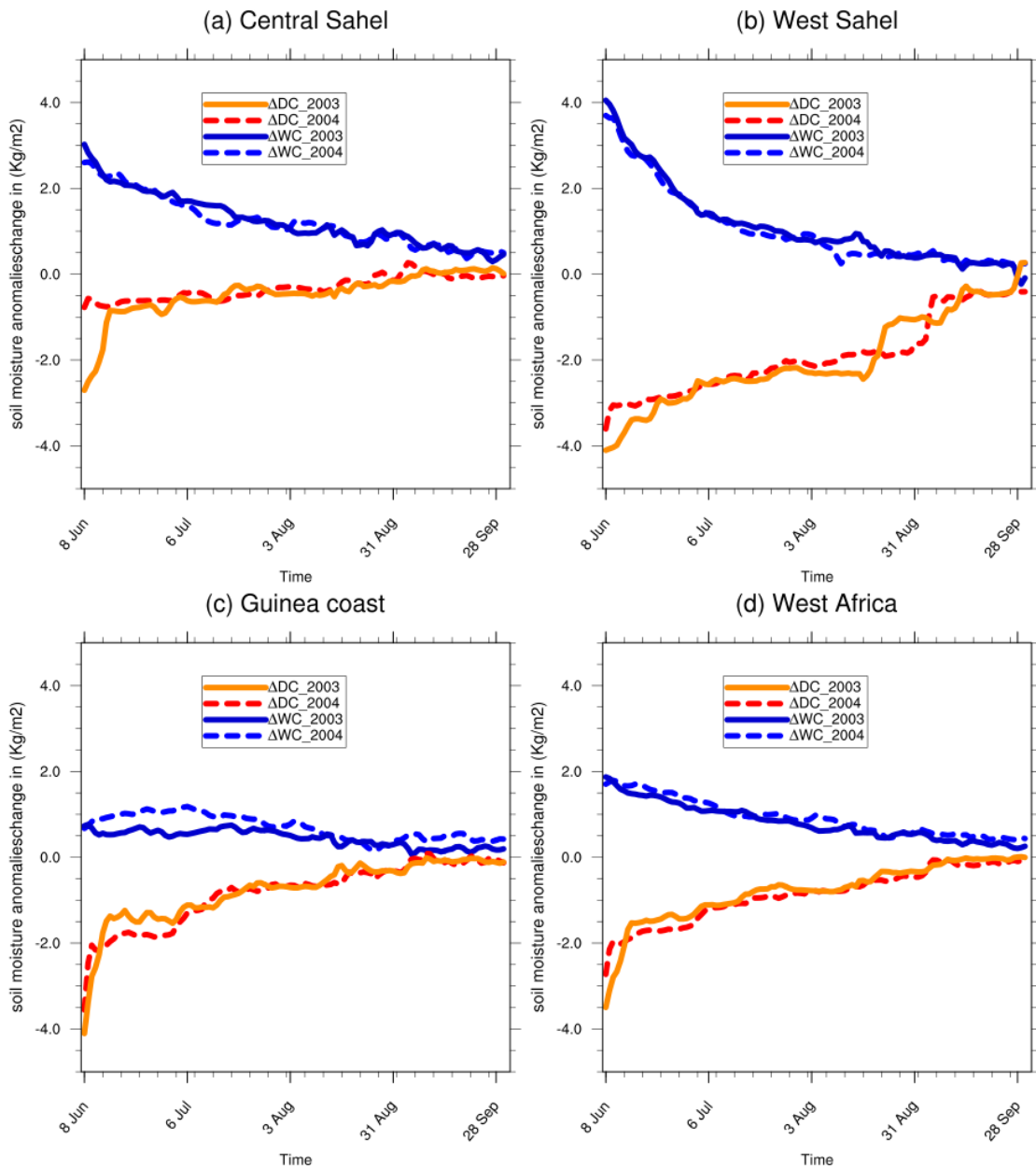
861

862

863

864

865



867

868 **Figure 6:** Daily domain-average soil moisture changes for JJAS 2003 and JJAS 2004, from dry
 869 (ΔDC) and wet (ΔWC) experiments with respect to their corresponding control experiment.

870

871

872

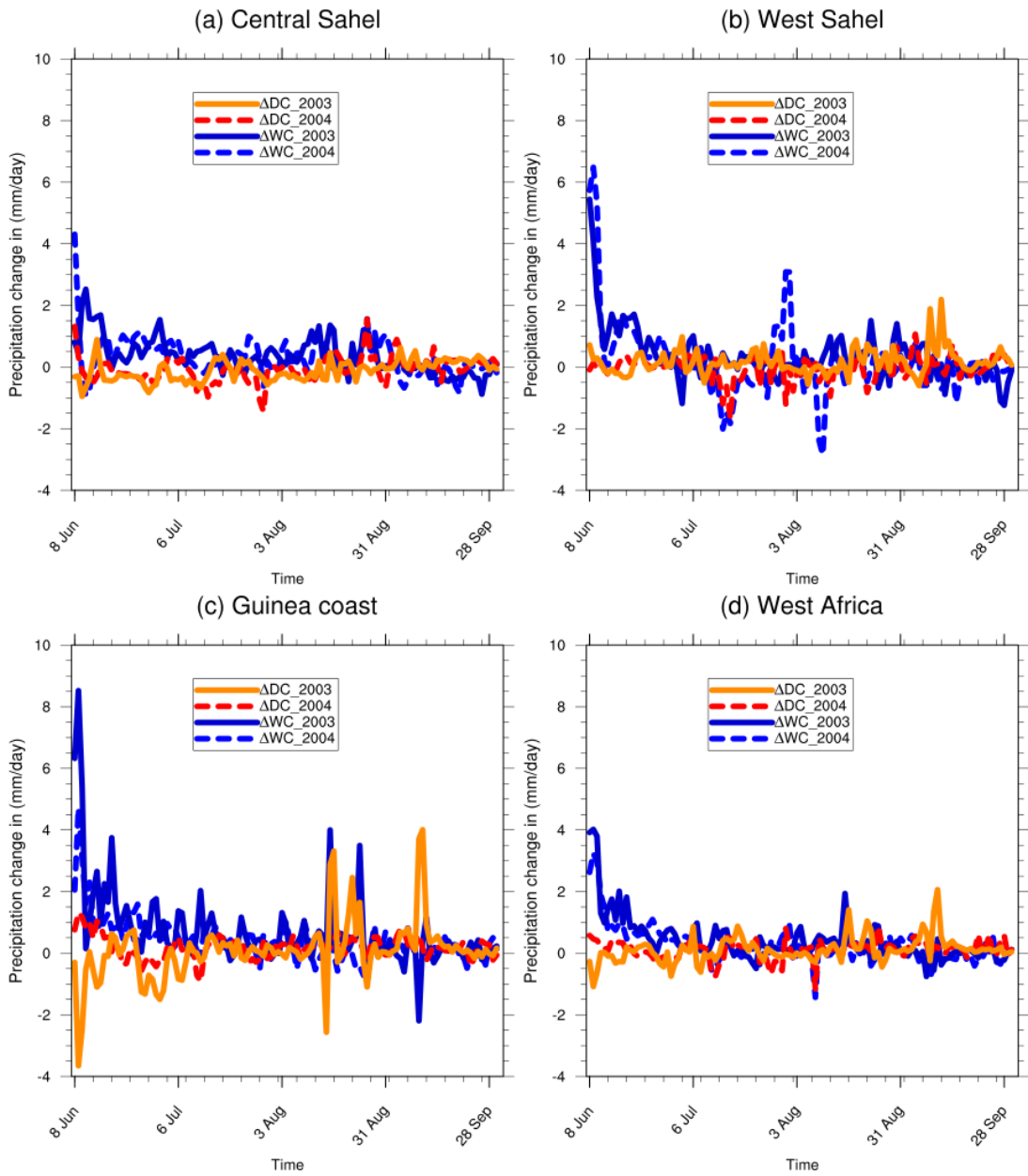
873

874

875

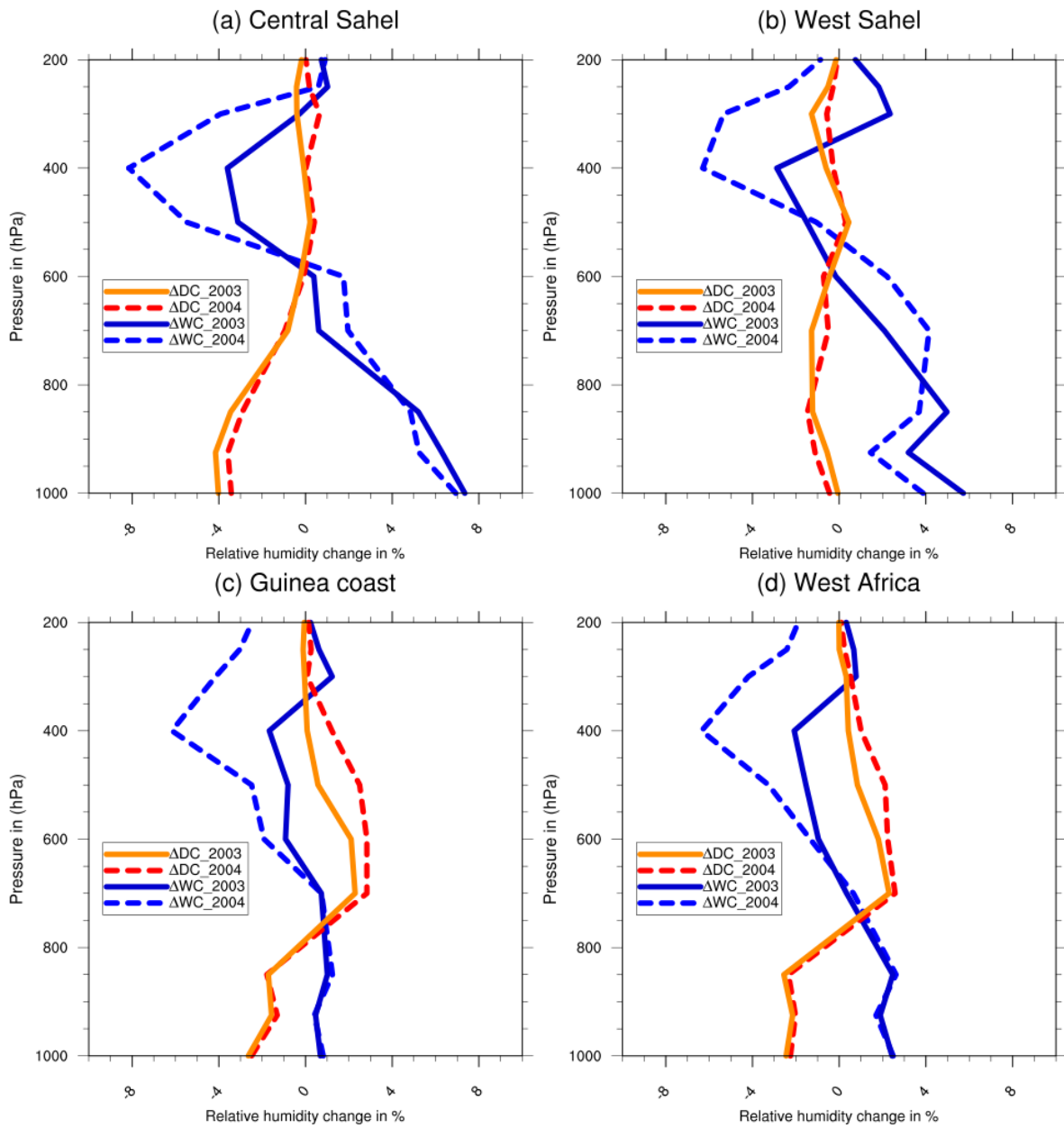
876

877



878
 879
 880
 881 **Figure 7:** Daily domain-average precipitation changes for JJAS 2003 and JJAS 2004, from dry
 882 (ΔDC) and wet (ΔWC) experiments with respect to their corresponding control experiment.
 883

884
 885
 886
 887
 888
 889



891

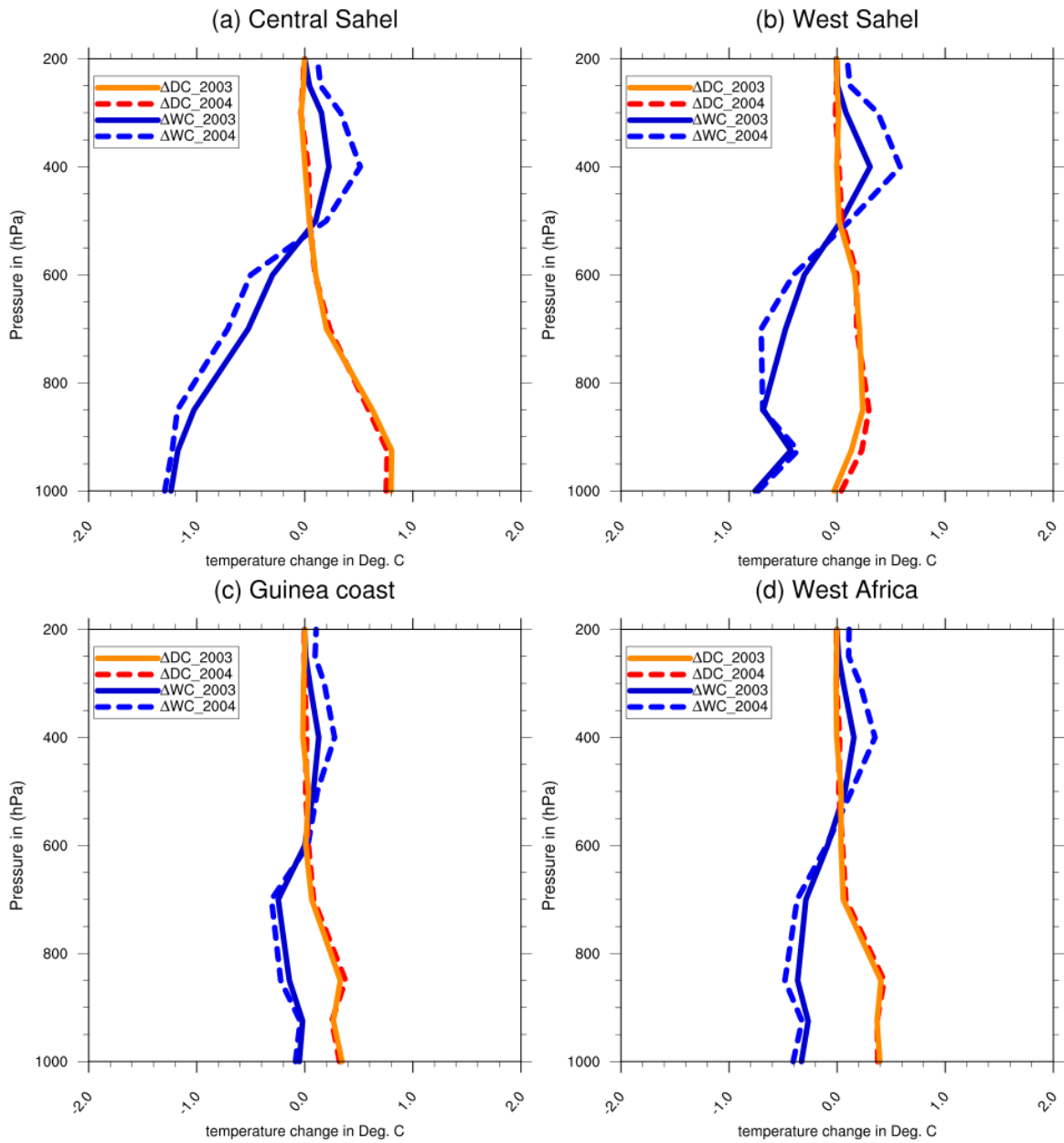
892

893

894 **Figure 8:** Vertical profile changes in Relative humidity for JJAS 2003 and JJAS 2004 from the
 895 dry (ΔDC) and wet (ΔWC) experiments with respect to corresponding control experiment over
 896 (a) central Sahel, (b) west Sahel, (c) Guinea coast, and (d) West Africa.

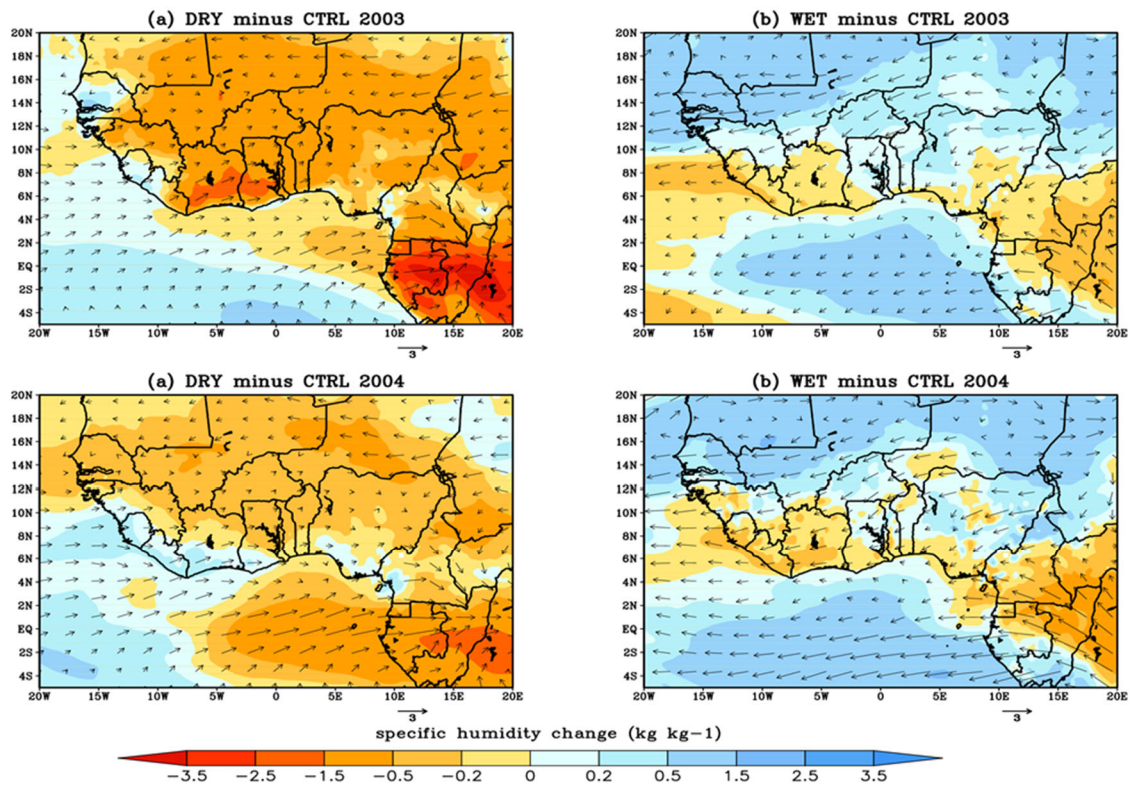
897

898



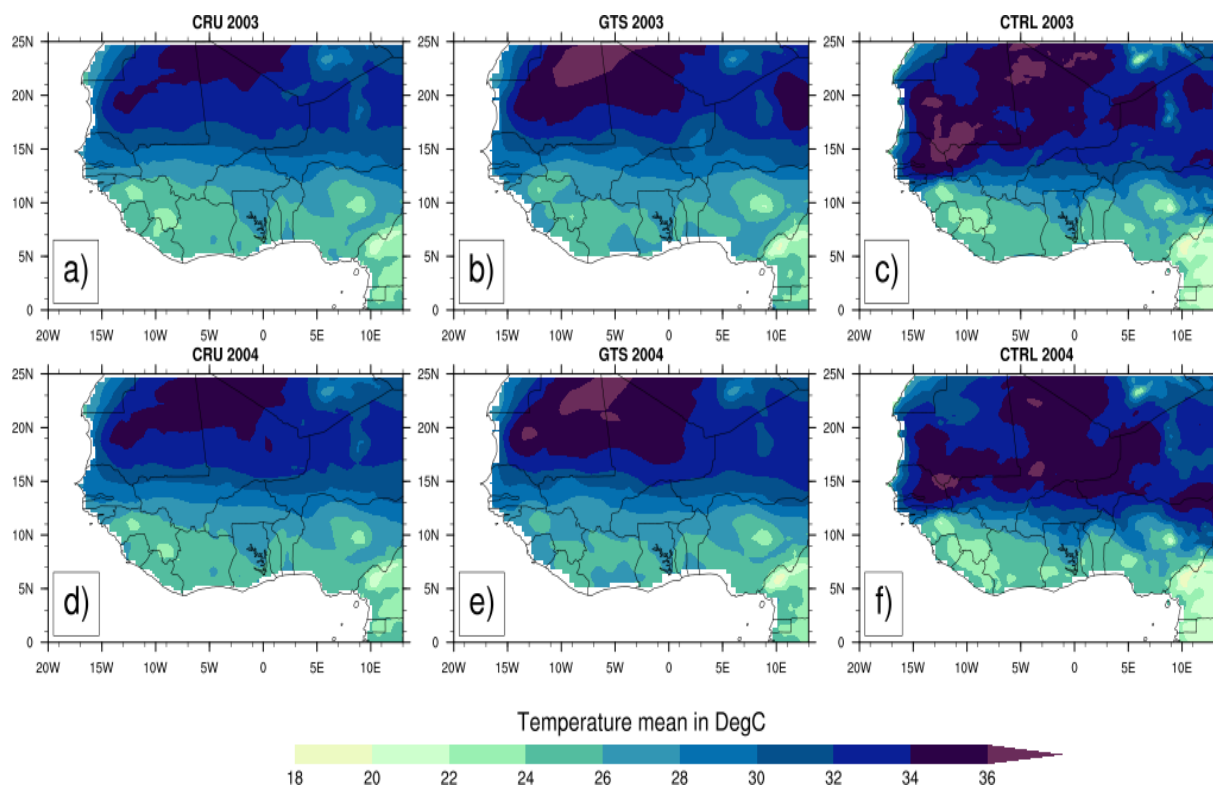
899
 900 **Figure 9:** Vertical profile changes in temperature for JJAS 2003 and JJAS 2004 from the dry
 901 (ΔDC) and wet (ΔWC) experiments with respect to their corresponding control experiment over
 902 (a) central Sahel, (b) west Sahel, (c) Guinea coast, and (d) West Africa.

903
 904



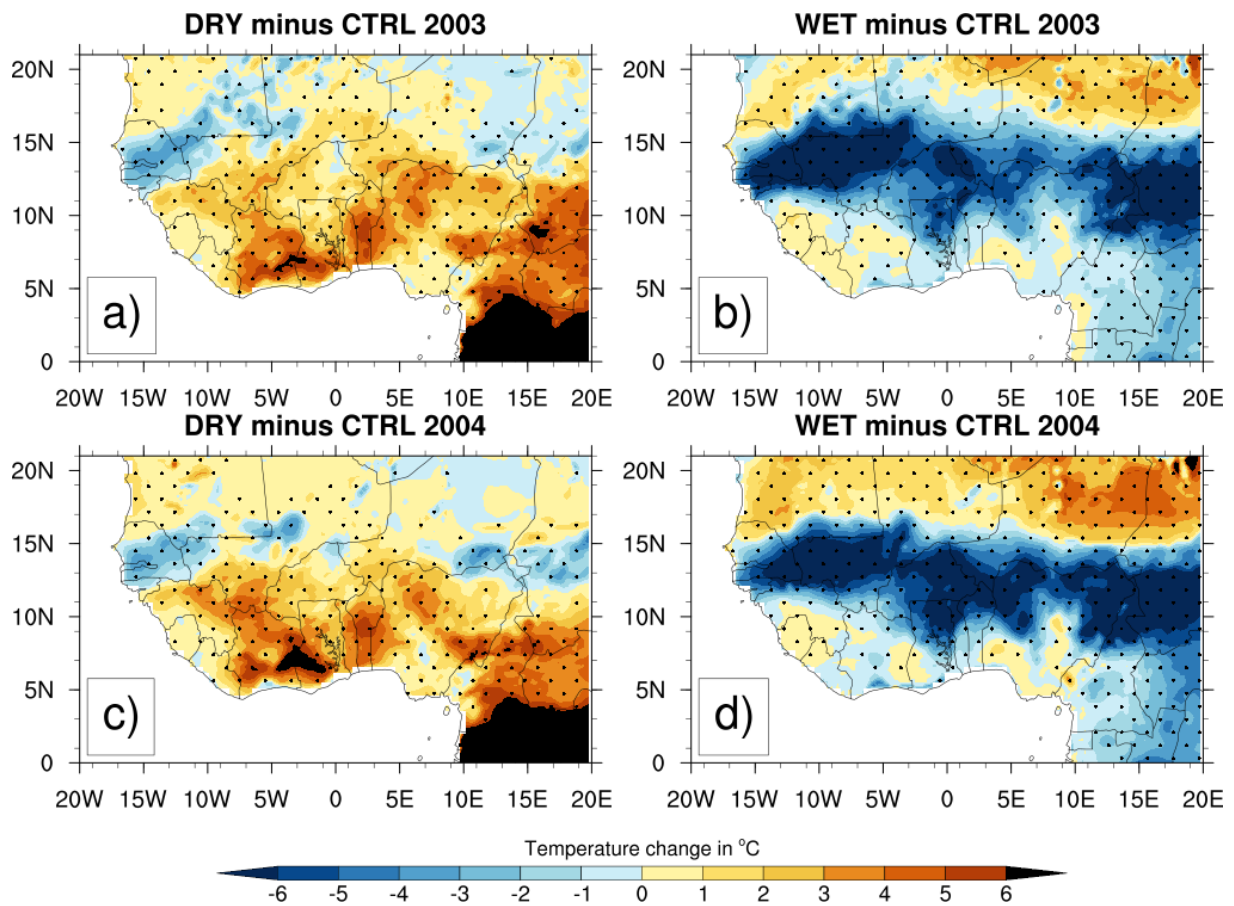
905
 906 **Figure 10:** The lower tropospheric wind (850hpa) and moisture bias for JJAS 2003 and JJAS
 907 2004 from the dry (a and c) and wet (b and d) experiments with respect to their corresponding
 908 control experiment.

909
 910
 911
 912
 913
 914
 915
 916
 917
 918
 919
 920
 921
 922
 923
 924



925
 926
 927
 928
 929
 930
 931
 932
 933
 934
 935
 936
 937
 938
 939
 940
 941
 942
 943
 944
 945

Figure 11: Observed 4-month averaged (JJAS) 2m-temperature ($^{\circ}\text{C}$) from CRU (a and d) and GTS (b and e) for 2003 and 2004 and their corresponding mean temperature simulated control experiment (c and f) with the reanalysis initial soil moisture ERA20C.



946

947

948 **Figure 12:** Changes in 2m-temperature (°C) for JJAS 2003 and JJAS 2004, from dry (resp. a and
 949 c) and wet (resp. b and d) experiments with respect to their corresponding control experiment,
 950 the dotted area shows differences that are statistically significant at 0.05 level.

951

952

953

954

955

956

957

958

959

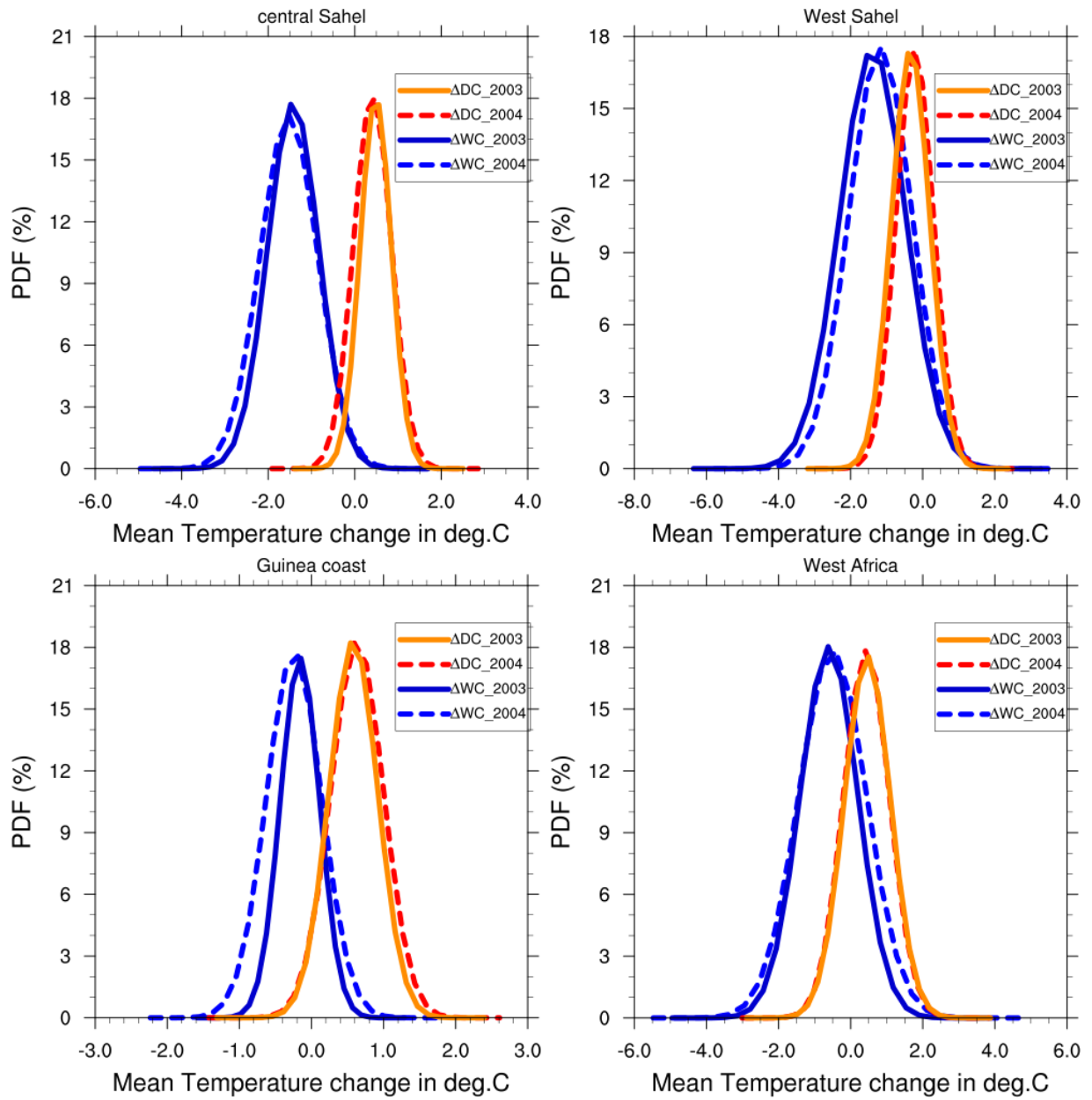
960

961

962

963

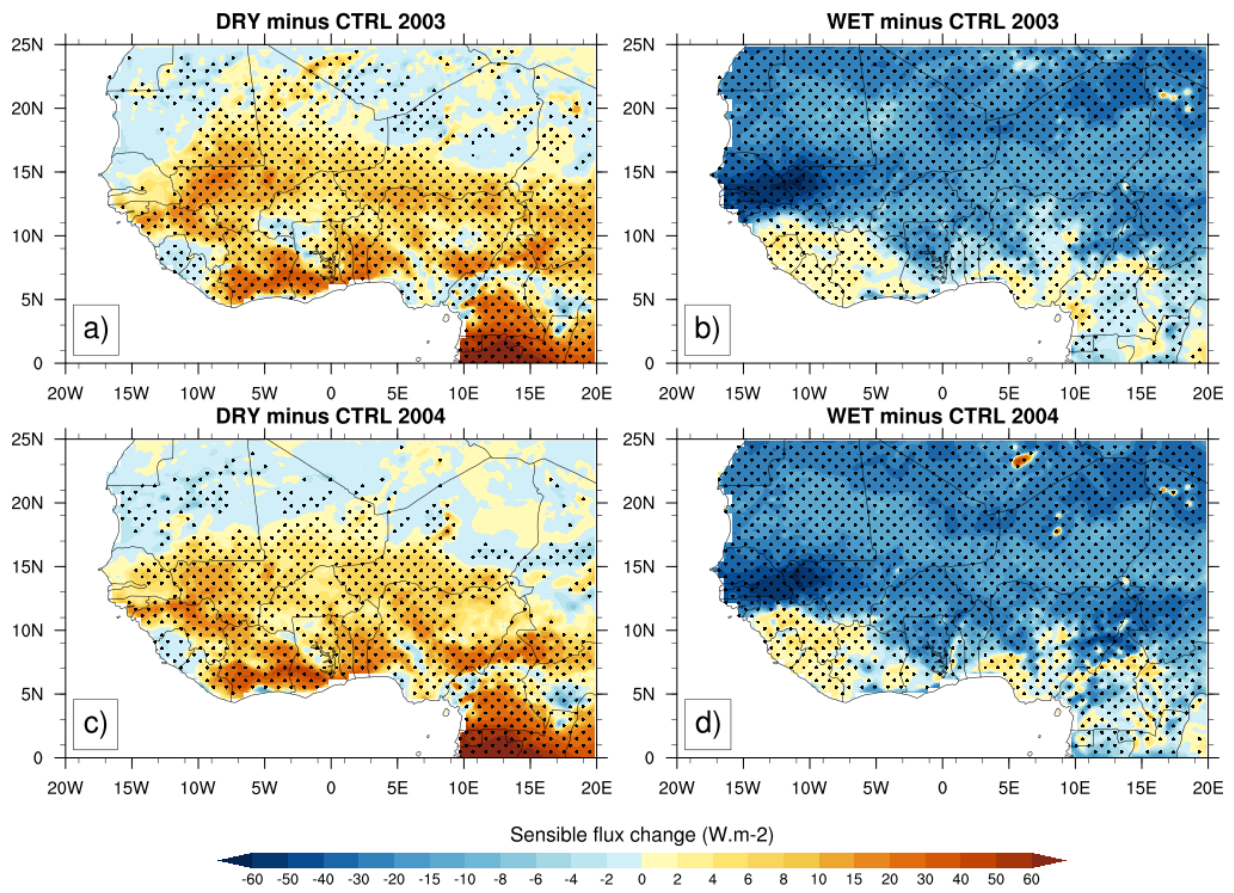
964



965
 966
 967 **Figure 13:** PDF distributions (%) of mean temperature changes in JJAS 2003 and JJAS 2004,
 968 over (a) central Sahel , (b) West Sahel, (c) Guinea and (d) West Africa derived from dry (ΔDC)
 969 and wet (ΔWC) experiments compared to their corresponding control experiment.

970
 971
 972
 973
 974
 975
 976

977



978

979

980 **Figure 14:** Same as Fig.12 but for sensible heat fluxes (in $W.m^{-2}$).

981

982

983

984

985

986

987

988

989

990

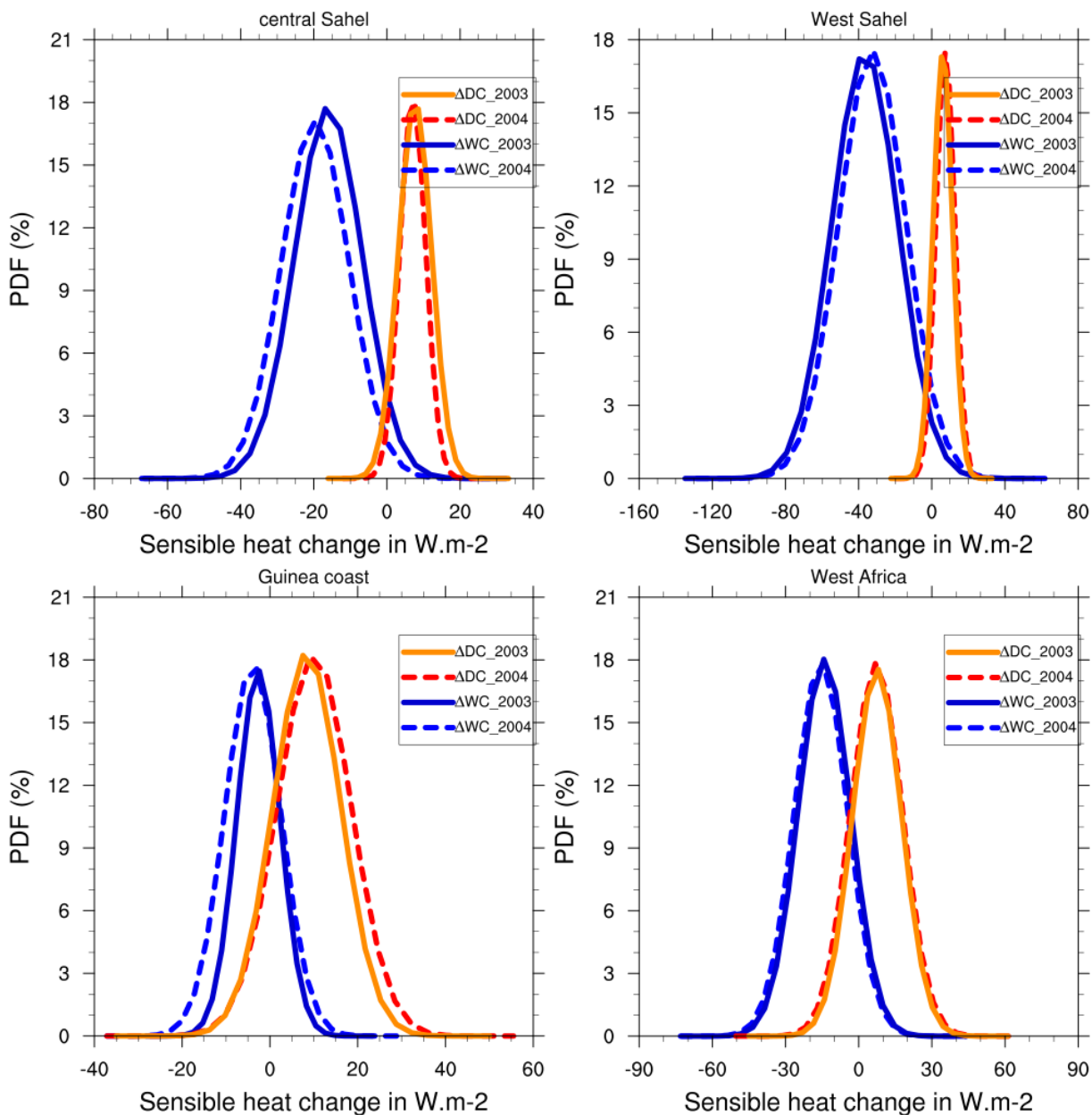
991

992

993

994

995



997

998

999 **Figure 15:** Same as Fig.13 but for sensible heat fluxes (in $W.m^{-2}$).

1000

1001

1002

1003

1004

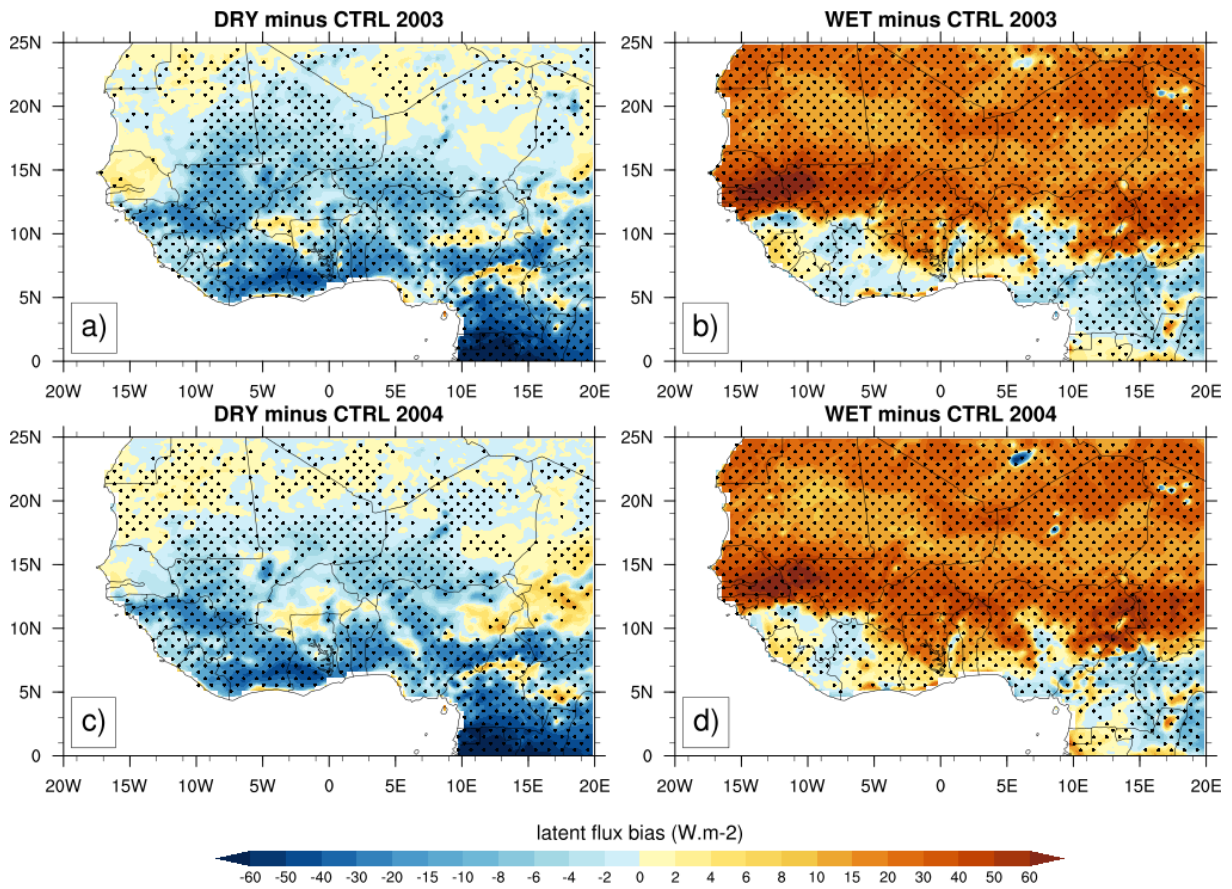
1005

1006

1007

1008

1009



1010

1011

1012 **Figure 16:** Same as Fig.12 but for latent heat fluxes (in $W.m^{-2}$).

1013

1014

1015

1016

1017

1018

1019

1020

1021

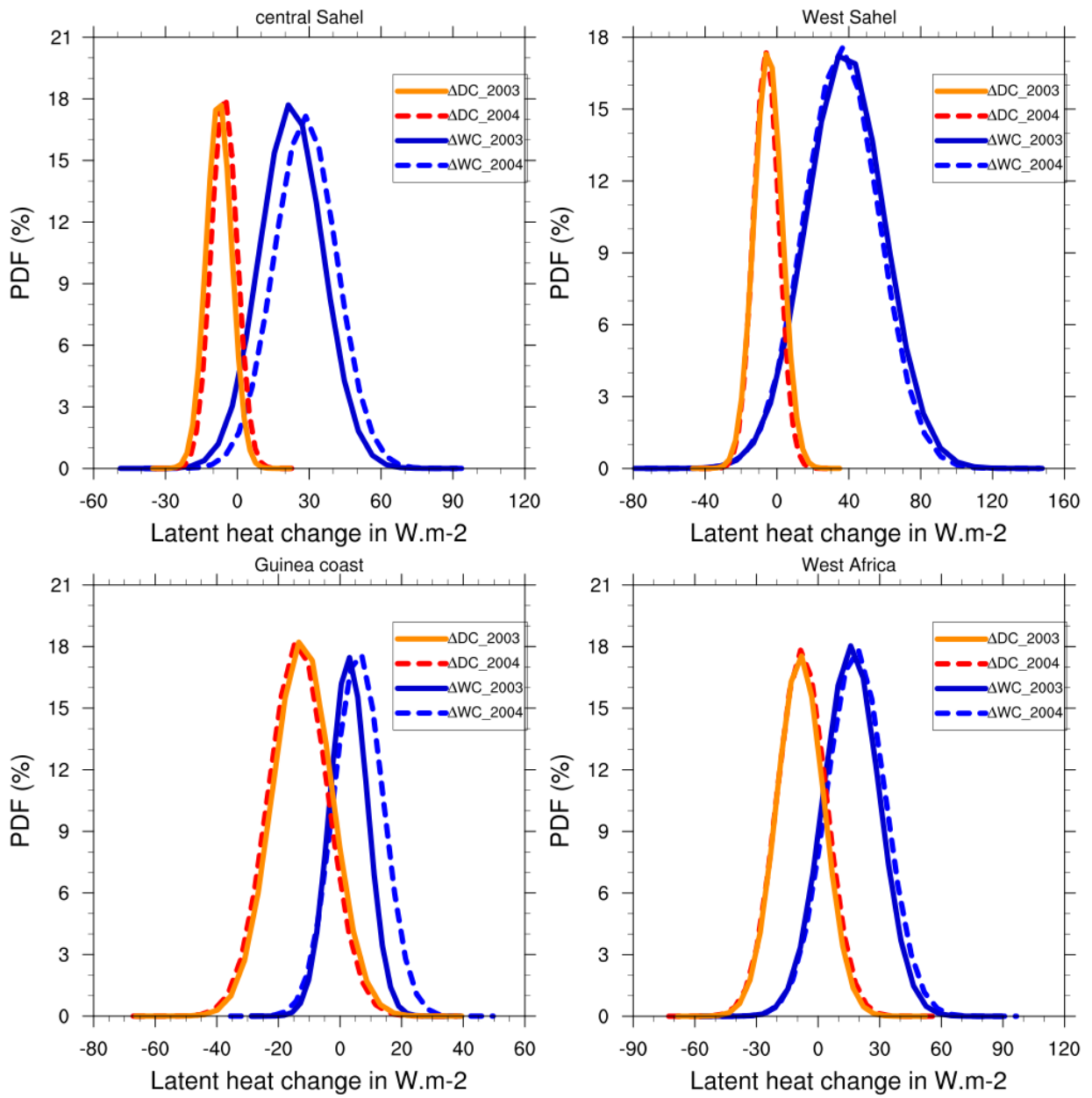
1022

1023

1024

1025

1026



1028

1029

1030

1031 **Figure 17:** Same as Fig.13 but for latent heat fluxes (in $W.m^{-2}$).

1032

1033

1034

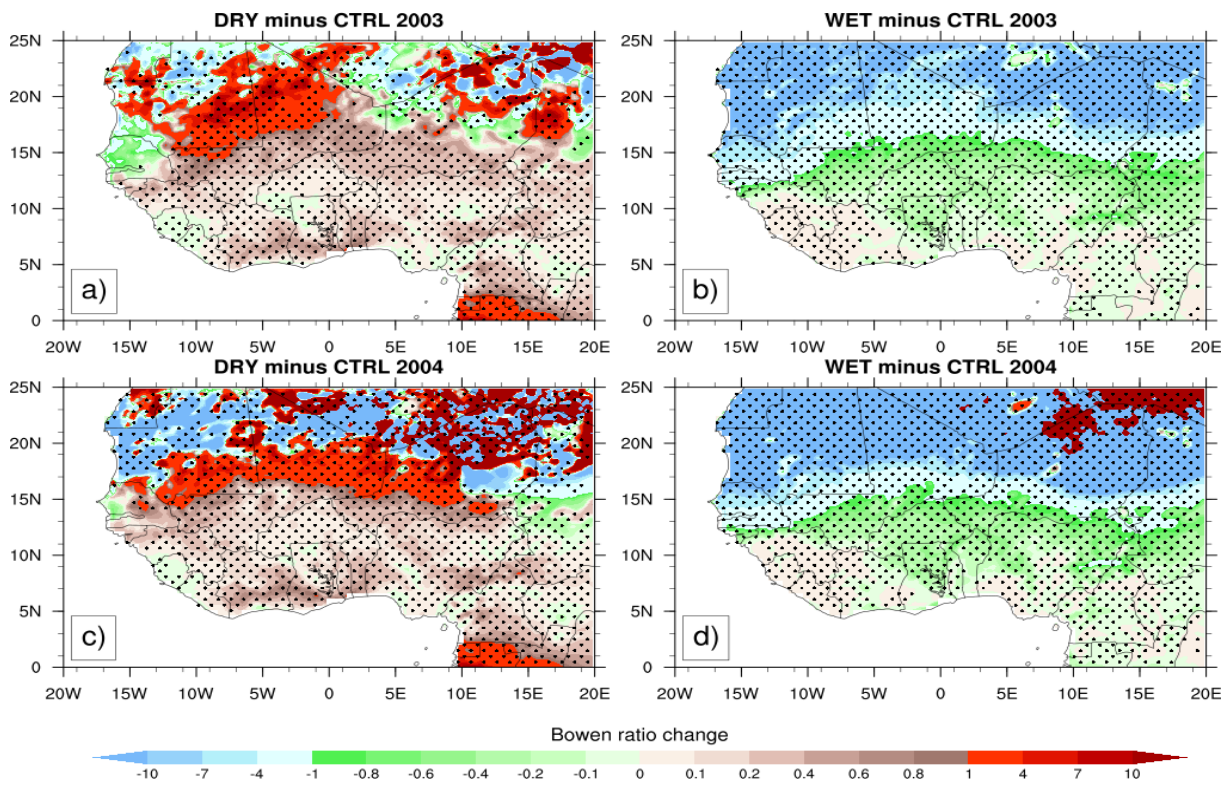
1035

1036

1037

1038

1039



1040

1041

1042 **Figure 18:** Same as Fig.12 but for Bowen ratio.

1043

1044

1045

1046

1047

1048

1049

1050

1051

1052

1053

1054

1055

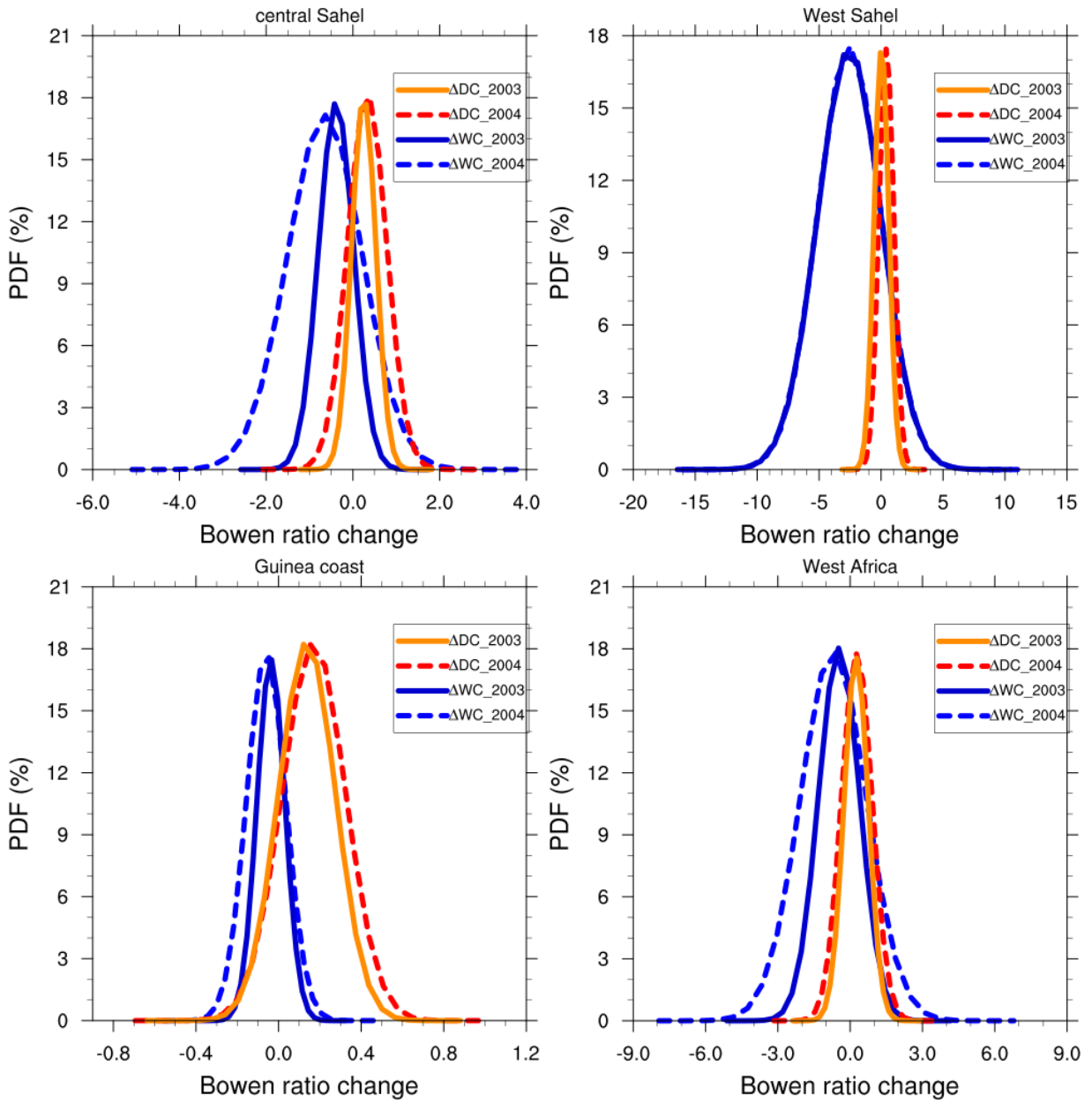
1056

1057

1058

1059

1060



1061

1062

1063 **Figure 19:** Same as Fig.13 but for Bowen ratio.

1064

1065

1066

1067

1068

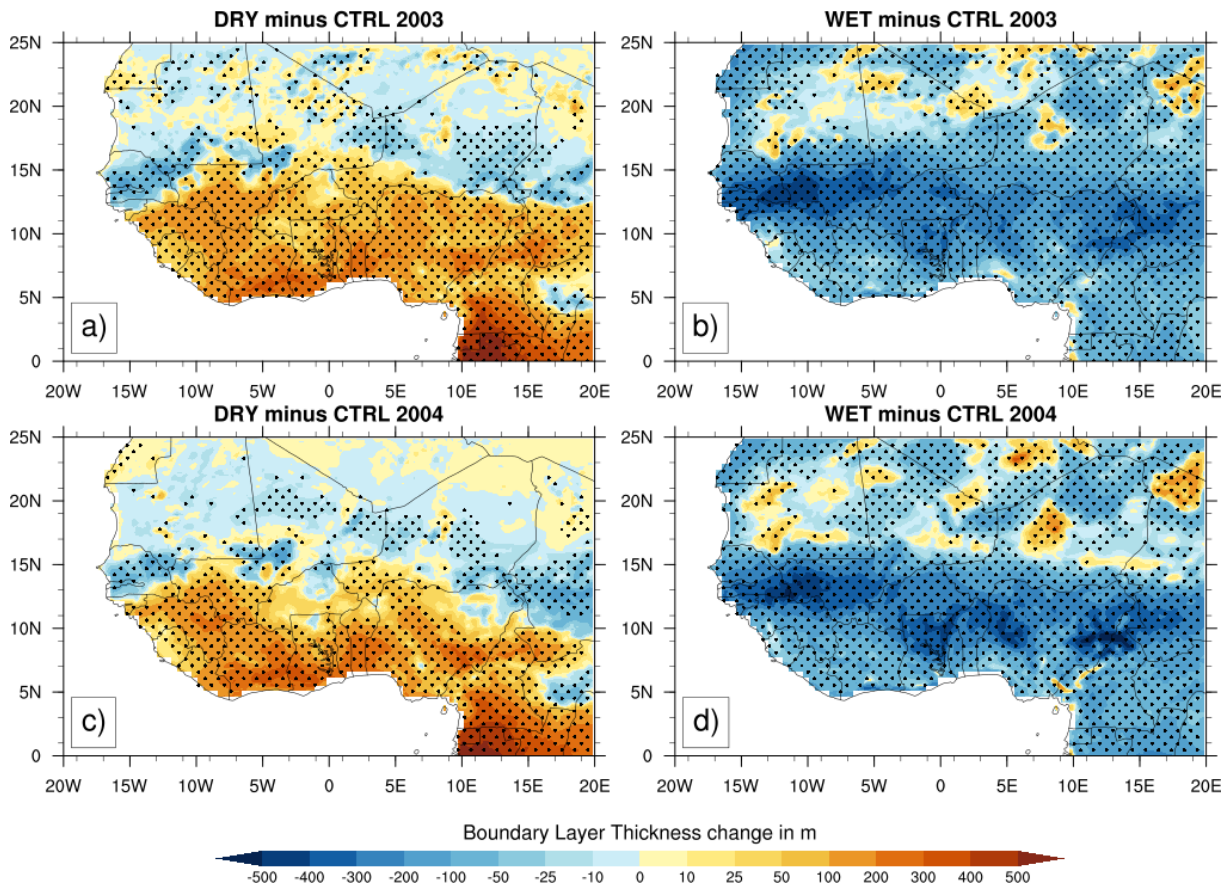
1069

1070

1071

1072

1073



1074

1075

1076 **Figure 20:** Same as Fig.12 but for the change of the height of the planetary boundary layer (in
1077 m).

1078

1079

1080

1081

1082

1083

1084

1085

1086

1087

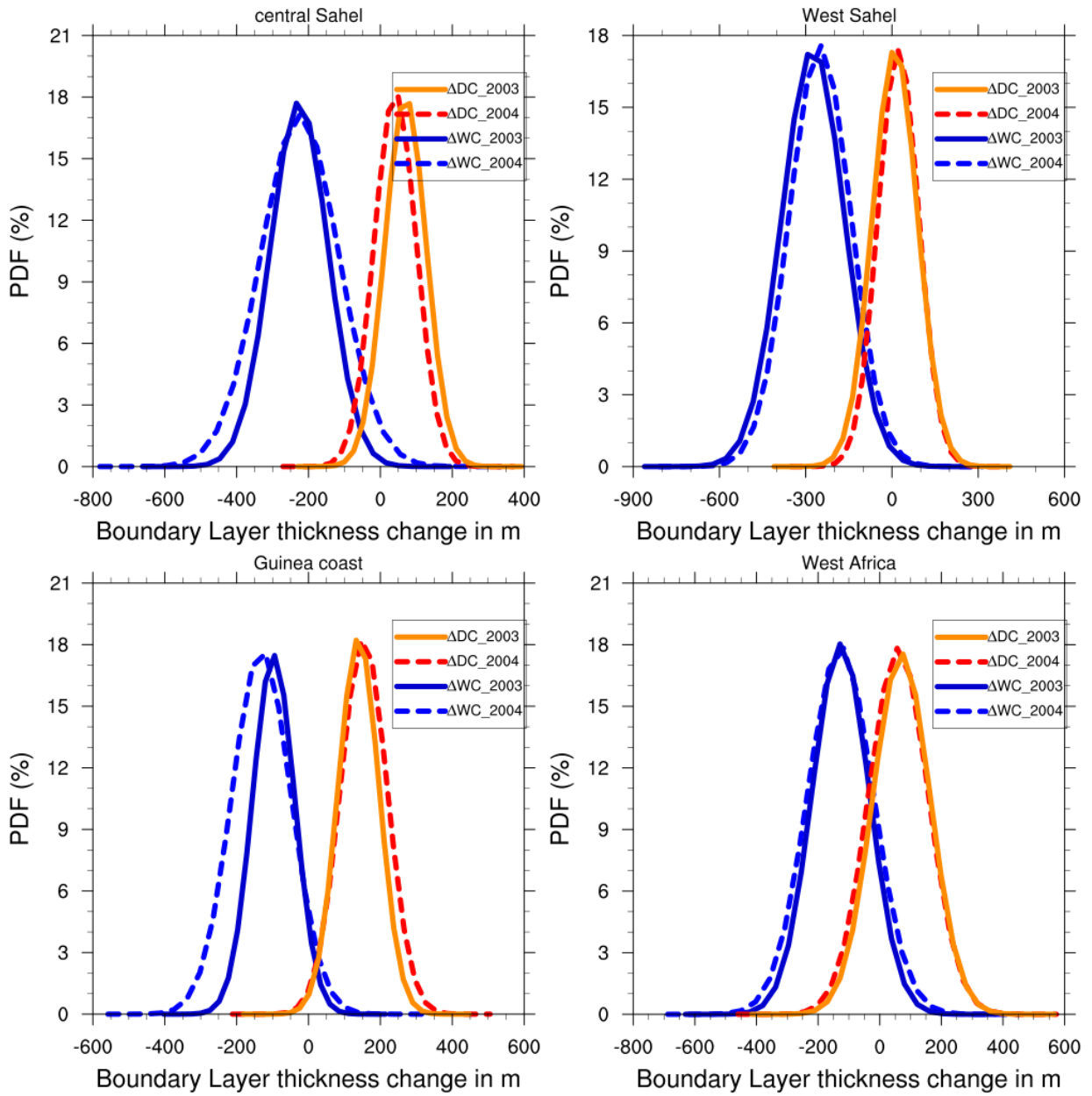
1088

1089

1090

1091

1092



1093

1094

1095 **Figure 21:** Same as Fig.13 but for the height of the planetary boundary layer (in m).

1096

1097

1098

1099

1100

1101

1102